The DNA damage response and RNA Polymerase II regulator Def1 has posttranscriptional functions in the cytoplasm

Akinniyi, O.T.[1, 2], Sebastian, A.[4], Kulkarni, S[1, 2], Hribal, M.M.[1,2], Keller, C.A.[3], Giardine, B.M.[1] Albert, I[1],[4] and Reese. J.C.[1, 2]

[1]Department of Biochemistry and Molecular Biology, [2]Center for Eukaryotic Gene Regulation and [3]Huck Institutes of the Life Sciences Genomics Research Incubator, [4]Huck Institutes of the Life Sciences, The Pennsylvania State University, University Park, PA, 16802 USA

* **Corresponding Author Address:**

Joseph C. Reese

Center for Eukaryotic Gene Regulation

Biochemistry and Molecular Biology

Penn State University

463A North Frear Laboratory

University Park, PA, 16802

Jcr8@psu.edu

(814) 865-1976

Running title: posttranscriptional functions of yeast Def1

Keywords: Def1, Ccr4-Not, ubiquitylation, translation, posttranscriptional control

Abstract:

Yeast Def1 promotes transcription elongation and RNA polymerase II degradation during genotoxic stress. Def1 is cytoplasmic, and DNA damage signals cause its proteolytic processing, liberating its N-terminus to enter the nucleus. Cytoplasmic functions for this abundant protein have not been identified. Proximity-labeling (BioID) experiments indicate that Def1 binds many proteins involved in posttranscriptional control and translation of mRNAs. Deleting *DEF1* reduces both mRNA synthesis and decay rates and directly tethering Def1 to a reporter mRNA suppressed expression, suggesting that Def1 directly regulates mRNAs post-transcriptionally. Surprisingly, we found that Def1 interacts with polyribosomes, which requires its N-terminal ubiquitin-binding domain and ubiquitylation of eS7a (Rsp7A) in the small subunit of the ribosome by the Not4 protein in the Ccr4-Not complex. Ribo-seq analysis revealed that deleting *DEF1* affected the translation efficiency of a specific subset of transcripts, a genome-wide shift in ribosome footprints on mRNAs and an increase in the dwelling of ribosomes at non-optimal codons. This, together with the high sensitivity of *def1Δ* to translation inhibitors further suggest impaired translation. The polyglutamine-rich unstructured C-terminus of Def1 is required for its interaction with decay and translation factors, suggesting that Def1 acts as a ubiquitin-dependent scaffold to link translation status to mRNA decay. Thus, we have identified a novel function for this transcription and DNA damage response factor in post-transcriptional regulation in the cytoplasm and establish Def1 as a master regulator of gene expression, functioning from transcription to translation.

Introduction:

Controlling gene expression and maintaining genomic integrity are intertwined and require coordinating multiple processes in the cytoplasm and the nucleus. One type of coordination is the phenomenon called gene expression buffering, whereby changes in mRNA synthesis in the nucleus are compensated by changes in mRNA decay in the cytoplasm(1–3). Sometimes, a factor initially identified for a function in gene expression in one cellular compartment is later found to participate in other control steps in another. For example, complexes and proteins that were known to affect transcription in the nucleus were later found to control posttranscriptional events in the cytoplasm(1, 2, 4, 5). These types of proteins are attractive candidates to explore how different stages in gene expression are coregulated. How coordination is achieved is unclear, but it involves either the shuttling of these regulators between the nucleus and cytoplasm or indirectly through feedback loops.

DNA damaging agents shut down multiple steps in gene expression, impacting transcription, mRNA decay, and translation. One response to damaged DNA is the ubiquitylation and degradation of the large subunit of RNA Polymerase II (RNAPII), Rpb1 (6–9). An essential protein in this process is yeast DEgradation Factor 1 (DEF1), first discovered as a protein co-purifying with the chromatin-bound transcription-coupled repair protein Rad26(10). Def1 binds arrested RNAPII and acts as a scaffold to initiate the recruitment of ubiquitin ligases and other factors used to degrade RNAPII(6, 8, 11). Def1 undergoes DNA damage and transcription stress-dependent proteasome-mediated proteolytic processing in the cytoplasm(6). The processing separates the N-terminus of the protein from the unstructured, polyglutamine-rich region located in the C-terminus that retains the protein in the cytoplasm. Def1 has nuclear functions, such as regulating TFIIH and transcription initiation, elongation, telomere maintenance, and multiple DNA repair pathways (8). Although much attention has been given to Def1's nuclear functions, it is a very abundant cytoplasmic protein. A major question is if Def1 has cytoplasmic functions or if its retention in this compartment only prevents it from interfering with RNAPII transcription in the nucleus under non-stress conditions. A hint of the former hypothesis is proximity labeling (BioID) experiments found that subunits of

Ccr4-Not deadenylase complex interact with Def1 and that the presumed human homology of Def1, UBPA2/2L, binds multiple cytoplasmic RNA binding proteins(12, 13).

Ccr4-Not was first identified as a transcriptional regulator in yeast, but it is now known to function at many points of gene control, including transcription, mRNA deadenylation, translation quality control and protein ubiquitylation(14–16). The complex is the major mRNA deadenylase that initiates degradation by polyA tail removal. We have shown that Ccr4-Not in the nucleus promotes transcription elongation and is essential for the DNA-damage-dependent destruction of the large subunit of RNA polymerase II, Rpb1, a function shared with Def1(5, 17, 18). Ccr4-Not's Not4 subunit is a~~n~~ RING domain ubiquitin ligase. The collection of substrates modified by Not4 is not known. One of the first proteins identified to be ubiquitylated by Not4 is eS7a (Rsp7a), a protein in the small subunit of the ribosome(19–21). It was later discovered that Ccr4-Not plays a role in co-translational degradation of poorly translated mRNAs, such as those rich in non-optimal codons. Arrest of the ribosome over a non-optimal codon in the A-site of the ribosome leads to the evacuation of the tRNA in the E-site, which is then filled by the N-terminus of the Not5 subunit of the complex. Then, Not4 ubiquitylates eS7a, and Ccr4-Not's deadenylase activity degrades the transcript(20). Although the Not4-dependent ubiquitylation of the small subunit is associated with translation quality control and co-translational decay, precisely what recognizes this modification and initiates these downstream events is unclear.

Here, we describe the cytoplasmic functions of yeast Def1. We demonstrate that Def1 binds many cytoplasmic proteins involved in posttranscriptional control of mRNAs, such as those involved in decay and translation. The loss of Def1 reduces mRNA decay rates globally, and a tethering reporter assay suggests that Def1 directly represses mRNA expression. We find that Def1 is associated with polyribosomes, which is dependent on its ubiquitin-binding domain and Not4-dependent ubiquitylation of the small subunit of the ribosome. We present evidence that suggests the C-terminus of Def1 recruits translation control and mRNA decay factors to the ribosome. Thus, we have identified a novel function for Def1 and uncovered a previously unknown consequence of ribosome protein ubiquitylation.

METHODS

Yeast strains and plasmids

Strains and plasmids used in this work are contained in Supplemental Tables 1 and 2, respectively. Gene deletions were produced by homologous recombination using PCR-generated cassettes(22). CUE domain mutants of *DEF1* were constructed using CRISPR-Cas9 gene editing as described(23). GFP fusion of Def1 were constructed as described in a previous publication(24). Genotypes of mutants were screened by PCR of genomic DNA and sequencing of PCR fragments.

Growth spot assay

Strains were grown at 30˚C to saturation in 5 ml of the appropriate medium. Serial dilutions were prepared in sterile distilled water, and diluted samples were spotted on plates containing the appropriate media and supplements. Plates were incubated at 30˚C for 24 hr or more, as indicated in the respective figures.

Auxin-inducible degron rapid depletion

Auxin-inducible degron (AID) strains were generated using plasmid constructs as previously used and described (25). Cells were grown to mid-log (OD600~0.5-0.6) phase in 1% yeast extract, 2% bacto-peptone, 2% dextrose supplemented with 20 ug/ml adenine sulfate (YPAD). Auxin (Indole-3-acetic acid, IAA) was added to a concentration of 500 uM for 2 hr. To monitor protein depletion was monitored by western blotting of proteins isolated by TCA extraction. with sterile distilled water. Proteins were isolated by TCA protein extraction.

Western blotting

Samples were separated on either SDS-PAGE or Tris-acetate gradient gels, and proteins were transferred unto nitrocellulose membranes by semi-dry transfer. Membranes were stained with ponceau S, imaged and de-stained. Membranes were blocked in 5% milk in TBST 50mM Tris-HCl, pH 7.5, 0.15M NaCl, 0.1mM EDTA, and 0.1% Tween-20) for at least 1hr and then probed with the primary antibody in 2% or 4% milk for at least 2 hr. Antibodies to Not1, Not4, Taf14 and Dhh1 are described in another

publication and were raised inhouse(13). Antibodies to Def1 were raised in rabbits to a 6HIS-Def1 (1-500) fusion. Commercial primary antibodies used are Anti-GFP (UBPbio, Y1031), Anti-FLAG M2 (Millipore Sigma) and anti-HA, (HA.11, Biolegend). Signals were detected by fluorescence or chemiluminescence (ECL) and imaged on X-ray film or a ChemiDoc-MP imaging system (Biorad).

BioID

Turbo ID (TID) was fused to the C-terminus of Def1, and truncation derivatives, using PCR-derived cassettes from pJR106 as described in (13). Free TID was expressed from the *CHA1* promoter, and this strain was used as the control. Protein extraction and isolation on streptavidin magnetic beads (Pierce, Thermofisher, #88817) was conducted as described in(13). Biological duplicates were analyzed. Proteins were digested on the beads with trypsin after alkylation with iodoacetamide. Purified peptides were labeled with TMTpro 16plex reagents (ThermoFisher, #A44520) per the manufacturer's recommended protocol. Details are found in (36).

RT-qPCR

RNA samples were quantified on Nanodrop and run on 1% agarose gel to confirm the quality. 1 ug of RNA was treated with 1U DNaseI for 30 min at 37˚C followed by quenching with 5 mM EDTA at 65˚C for 10 min. RevertAid RT kit (Thermo-Fisher,FERK1622) was used for cDNA preparation according to the manufacturer's protocol using a mix of random and oligo dT primers. Serial dilutions of cDNA were used to set up qPCR reactions. PCR reactions were performed with PerfeCTa SYBR green SuperMix and using an Agilent Real-Time machine. The data was analyzed using the Agilent AriaMx software and Excel.

Total RNA-seq for steady state mRNA levels

Cells were grown in YPAD and harvested at log phase (OD600~0.8-1). Cells were washed with nuclease-free water and resuspended in AE-buffer (50 mM sodium acetate pH 5.3, 10 mM EDTA). Cells were spiked with *S. pombe* cells at a ratio of 14:1. RNA was isolated using AE-phenol chloroform extraction, followed by overnight ethanol

precipitation with sodium acetate. RNA samples were washed with 80% ethanol and resuspended in nuclease-free water. RNA was quantified on Nanodrop, and the quality was verified by analysis on a Tapestation. RNA samples with RIN scores >9.0 were used. Biological replicates were analyzed.

RNA metabolic labeling studies

The procedure is a derivative of that used in a previous publication(26). *Saccharomyces cerevisiae* cells growing in YPD were treated at log phase (OD_{600}~0.8-1) for 6-, 9-, 12-, 24- and 90-min with 0.65mg/ml 4-thio-uracil (Millipore-Sigma). Thirty OD_{600} cultures were transferred to 2 volumes ice-cold methanol on dry ice to halt 4tU incorporation. Cells were harvested by centrifugation at 3000 rpm for 3 min, and resuspended in AE-buffer (50 mM sodium acetate pH 5.3, 10 mM EDTA). The *S. cerevisiae* cells were spiked with pre-labeled *S. pombe* cells at a ratio of 1:14. *S. pombe* spike-in were generated by growing cells in YPD to log phase (OD_{600}~0.8) and treated with 50 uM 4tU for 12min. RNA was isolated using AE-phenol, then chloroform, followed by overnight ethanol precipitation. RNA samples were resuspended in nuclease-free water. RNA was subjected to biotinylation (120 ug RNA, 20 mM HEPES pH 7.4, 12 ug MTSEA biotin-XX (Biotium Co) in 600 ul final volume for 30 min at room temperature. Free MTS-biotin reagent was removed by PCIAA-extraction and precipitation with NaCl and isopropanol. Dynabead MyOne streptavidin C1 beads were washed twice in high salt wash buffer, HSWB, (100 mM Tris-HCl pH 7.4, 10 mM EDTA, 1M NaCl) and blocked with blocking buffer (100 mM Tris-HCl ph7.4, 10 mM EDTA, 1M NaCl, 40 ng/ul glycogen), then resuspended in HSWB. 80 ug of biotinylated RNA was incubated at 65°C for 7 min and streptavidin pull down was performed using 100 ul blocked beads and then washed thrice with HSWB, and eluted twice in 25 ul elution buffer (100 mM DTT, 10 mM EDTA, 1M NaCl, 0.05% Tween-20). The RNA was concentrated and quantified on a Qubit instrument (Life Technologies).

Library preparation and NextGen sequencing

Total RNA was depleted of rRNA using the Qiagen FastSelect (#334215) kit. Libraries for steady-state RNA and RATE-seq samples were prepared using the

Illumina Total Stranded library prep kit and the Illumina UDI indexes (#20040529). The libraries were analyzed on TapeStation-4150 at the Genomics Core Facility, Penn State University, and were quantified using NEBNext® Library Quant Kit for Illumina®. Libraries were sequenced on the Illumina NextSeq 2000. Illumina P2 100 cycle reagent cartridge (#EC1591461-EC11) was used for paired-end sequencing. Reads were mapped to the sacCer3 genome using the ENCODE 3 pipeline. Spike-in reads were mapped to the *S. pombe* genome (https://www.encodeproject.org/pipelines/ENCPL002LPE/). Star was used to map the reads, and RSEM-1.2.28 to get estimated counts and TPMs (Genes: Saccharomyces_cerevisiae.R64-1-1.106.ucsc.gtf). DESeq2 was used to determine the differential expression of genes(27). The truncated expected counts from the RSEM output were used as input for DESeq2. Genes with <15 reads across samples were filtered out. The p_{adj} value of 0.01 was used as a threshold.

RATE-seq data modeling

RNA reads obtained from Deseq2 were used for nonlinear regression modelling to obtain decay rates in *R* using the *nls.table* function. The model for RNA decay is (28):

$$Y_t = Y_{eq}\left(1 - e^{-(\propto_{RNA} - \propto_{growth})(t - t_d)}\right)$$

Where

Y_t = Amount of labelled transcript at time *t*

Y_{eq} = Abundance of labelled transcript at steady state

t = labeling time

t_d = delay time

RNA decay rate constant, $\propto = \left(\propto_{RNA} - \propto_{growth}\right)$

α_{RNA} = RNA decay rate

α_{growth} = Growth rate = *ln2/doubling time* = 0.0077 (WT) or 0.0046

Synthesis rate was estimated in Excel from decay rate constant using the formula:

$$Synthesis\ rate = \propto\ [mRNA]$$

Where mRNA abundance estimated from steady state read counts assuming a total of 60000 mRNA molecules per cell(29).

mRNA half-life was estimated in Excel from decay rate constant using the formula:

$$Halflife = \frac{ln2}{\propto}$$

Polysome profiling

Fifty ml of mid-log-phase cultures were treated with 100ug/ml cycloheximide for 10min. Cells were harvested by centrifugation at 4000 rpm for 5 min. Lysate preparation was carried out as previously described(19). Cells were resuspended in 500 ul polysome buffer with cycloheximide (CHX) and protease inhibitors (20mM HEPES-OH pH 8, 10 mM $MgCl_2$, 50 mM KCl, 1% triton X-100, 1 mM DTT, 100 ug/ml CHX, 1 mM PMSF, 0.5 ug/ml leupeptin, 1 ug/ml pepstatin) followed by the addition of 500 ul glass beads. Cells were broken by shaking for 18 min on a vortex mixer at 4˚C (3 cycles of 6 min bead-beating and 5 min of cooling on ice). Lysates were centrifuged for 10 min at 14,000 rpm and the protein concentration of the clarified supernatant was quantified by Bradford assay. Extracts were stored at -80°C until use. Continuous 10-50% sucrose density gradients (SDG) were prepared on GradientMaster (Biocomp) and stored at 4°C for at least 1hr. 1 mg of protein equivalent of lysate was layered onto the SGD and centrifuged at 39k rpm for 2.5 hr in a SW40 rotor (Beckman Coulter). SDG was fractionated on a Brandel fractionator and the OD254 of peaks were recorded by *PeakChart 3*. Samples used for Western blotting were prepared by precipitation with 10% TCA in the presence of 10 or 20 ug of BSA overnight at 4°C. The precipitated proteins were collected by centrifugation at 14k rpm for 10 min and the pellet was washed with 100% acetone. Proteins were solubilized in 1X SDS-PAGE loading buffer and boiled for 5min. Western blotting was performed as described above.

Riboseq and data analysis

Ribo-seq was conducted as described previously (30, 31) in triplicate (biological). After library preparation 50bp paired-end reads were sequenced. Using fastp, we

trimmed the Illumina universal adapter sequence and low-quality bases from the data. Reads with a minimum length of 20bp were retained. Samples were split into replicates based on barcode sequences. Data was mapped to the yeast genome using hisat2 and the RPF read counts at coding sequence (CDS) of each gene was obtained with featureCounts. The CDS raw RPF read counts were used for differential expression analysis. We studied the ribosome profiling features using RiboMiner v0.2. Transcript sequences were prepared using the prepare transcript command in RiboMiner, and Read1 data was mapped to the transcripts using bowtie2. Frame distribution, length distribution and periodicity were checked. Based on the periodicity plots, only 28bp long reads were used for further analysis. P-site was estimated to be at 12 bp offset from the 5 bp end of 28 bp long reads. Metagene analysis was performed, and plots were generated for the whole transcript region and also for 500bp region from CDS start and end. Polarity values were computed to judge whether the ribosome density is enriched at the 5' end or the 3’ end. Additionally, codon density at A-sites and P-sites was calculated and plotted.

Deseq2 was used to model the RPF and RNA-seq read counts in a generalized linear model (GLM). Genes with significant changes in translational efficiency were obtained using DESeq2 following the DeltaTE approach.

mRNA decay and transcription reporter assays

The MS2-MCP mRNA reporter assay was conducted as described in a previous publication(32). Plasmids expressing MCP fusions with Def1, or fragments of the Def1 coding sequence, were constructed from gene synthesis and PCR-generated fragments using inPhusion assembly (Takara Bio) (Supplemental Table 2). MCP fusion protein expression plasmids were co-transformed with the reporter vector pJC428 into W303 cells (Supplemental table 1). Cells (triplicates) were grown in triplicate in -uracil/-leucine dropout media containing 2% galactose to an OD_{600} of 1.0. Each sample was split into two, one used for protein extraction, and the other for RNA extraction. Expression levels of the MCP fusion proteins were verified using anti-FLAG antibodies and the levels of reporter GFP protein using anti-GFP antibodies. To calculate the levels of GFP protein, a serial dilution standard curve of an extract was included on the blots. Loading was

normalized to Taf14 levels, which served as a loading control. GFP mRNA was measured by qPCR and normalized to *ACT1* mRNA.

The Beta-galactosidase transcription reporter assay was conducted by co-transforming W303 cells with pSH18-34 and plasmids expressing LexA fusion proteins with Def1 (Supplemental Table 2). Cells were grown in triplicate in -uracil/-leucine dropout media containing 2% dextrose to an OD_{600} of 1.0. Protein extraction and beta-galactosidase assays were conducted as described in another publication(33).

Results:

Def1 affects steady state RNA levels and RNA metabolism rates

Def1 regulates elongation, especially removing arrested RNA polymerase II during transcription stress(6, 8). Although Def1 regulates RNAPII activity, no analysis of the effect of deleting *DEF1* on transcription has been described. We carried out RNA-seq in wildtype and *def1*Δ mutant strains. 6486 RNAs were detected, which include all types of RNA. Using a cutoff of >2-fold change and a $p_{adj}<0.01$, 612 and 475 transcripts were observed to be downregulated and upregulated, respectively (Fig. 1A and Supplementary file 1). All differentially expressed transcripts were mRNAs. These differentially expressed genes were subjected to GO term analysis, and genes that were upregulated are associated with ribosomes and translation. Transcripts downregulated in the mutant were related to carbohydrate metabolism and metabolic pathways (Supplementary Fig. S1A-D).

RNA-seq measures steady state RNA level, which is a function of synthesis and decay of transcripts. Studies have shown that cells alter one pathway to respond to changes in the other called transcript buffering(1, 4). We therefore investigated transcript synthesis and decay rates in the *def1*Δ mutant. We employed RNA-approach-to equilibrium (RATE-seq), a pulse-only metabolic labeling approach whereby cells are treated with 4-thiouracil for increasing labeling times as incorporation of the nucleoside analog approaches equilibrium(28). 4-ThioU-labeled *S. pombe* RNA was used as a spike-in control (see Methods section). We carried out RATE-seq in wild type and *def1Δ* cells and estimated synthesis and decay rates for 3938 and 5631 transcripts,

respectively. We next analyzed the median synthesis and the decay rates of the 3596 transcripts that were common to both the wild type and mutant data sets. The synthesis rate of mRNAs was repressed globally in the mutant. The median synthesis rate was about 3.7-fold lower in the mutant than in wild type cells, but the change in synthesis for some transcripts was significantly higher (Fig. 1B and Supplementary file 2). Considering that global synthesis rates were repressed, yet a few transcripts showed differential expression, this suggested that RNA destruction rates were reduced to compensate for this change. We calculated the decay rates and RNA half-lives and found that the median decay rate in wild type cells under our conditions was 0.259/s, which corresponds to a median half-life of 2.7 min (Fig. 1C and Supplementary Fig. S2A). The half-life value we estimated is shorter than some reported measurements, but the values of median mRNA half-life from other studies varied between 2-18 minutes and is highly dependent on methodology and labeling conditions (Supplementary Fig. 2B). Most importantly, the decay rate was 3.2-fold lower in the mutant, indicating a stabilization of mRNAs (Fig. 1C).

If Def1 regulates RNAs of genes involved in specific cellular processes or pathways, we would expect that its effects on half-lives would be most pronounced in such transcripts. To determine if Def1 targets mRNAs within specific pathways, we subjected transcripts in the top quartile of half-life fold change to GO term analysis. The biological process of mitochondrial translation, protein metabolism and translation were highly represented as targets of Def1 (Fig. 1D).

We next plotted the change in decay rates of individual mRNAs versus their change in synthesis rates (Fig. 1E). A strong correlation was observed (R=0.834), indicating that transcript buffering is occurring in the mutant. This suggests that *DEF1* is not required for transcript buffering.

Def1 interacts with RNA regulation factors

Proximity labeling, BioID, is used to identify protein-protein interaction in cells and allows for the detection of transient and weak interactions(34, 35). Recently, we conducted BioID on subunits of the Ccr4-Not complex and found that multiple bait proteins strongly labeled Def1(13). Furthermore, the human homolog of Def1,

UBAP2/2L, interacted with hCcr4-Not subunits(12, 36). Therefore, we conducted the reciprocal experiment of performing BioID on Def1, fusing the TurboID (TID) version of the enzyme to the C-terminus (37). We expressed “free” TID to levels close to that of Def1-TID as a control and calculated the fold increase in the biotinylation of targets (Def1-TID versus free TID). We subjected the labelled proteins to mass spectrometry and then used a cutoff of 1.5-fold enrichment and $p<0.05$ to identify interacting or proximal partners of Def1 (Fig. 2A and Supplementary file 3). 93 proteins met these criteria, of which 34 are involved in some aspect of RNA regulation. We submitted the enriched proteins to GO term analysis, which returned terms associated with the regulation of translation, post-transcriptional control and mRNA decay and the component terms ribonucleoprotein granule, P-body, translation initiation factor 4F, polysome and the Ccr4-Not core complex (Fig. 2B and 2C).

It was quite surprising that many RNAPII transcription factors or other nuclear proteins involved in mRNA synthesis were not labelled by Def1. This could be explained by Def1’s localization in the cytoplasm in the absence of transcription stress. Furthermore, the biotin ligase was fused to the C-terminus of Def1 and the C-terminus maintains Def1 in the cytoplasm (6). This data indicates that Def1 interacts with cytoplasmic RNA regulating proteins and suggests that it has posttranscription functions such as mRNA storage, translation or decay.

Directly tethering Def1 to mRNA suppresses expression, suggesting a role in posttranscriptional control

The extended half-lives of mRNA in the *def1*Δ mutant and the labeling of many mRNA regulators by Def1-TID suggests it regulates mRNAs in the cytoplasm. However, the reduced mRNA turnover could be a compensatory response to the lower synthesis rate due to transcript buffering (3), which confounds making the conclusion that Def1 directly regulates mRNA. Next, we used an MCP/MS2 tethered reporter, which has been used to demonstrate direct regulation of mRNA by decay factors(32). The reporter construct produces an mRNA with a green fluorescent protein (GFP) ORF and MS2 stem loops in the 3’ UTR (Fig. 3A). MCP was fused to either the N- or C-terminus of Def1 (MCP-DEF1 and DEF1-MCP respectively), and both were analyzed to rule out

position effects. The *DEF1-MCP* fusion proteins fully complemented a *def1Δ* strain, indicating the fusion proteins were functional (Supplementary Fig. S3A). Both Def1-MCP fusion proteins were expressed to equal levels as the free MCP protein (Supplementary Fig. S3B). A Dhh1-MCP fusion was used as a control, since it represses this reporter mRNA(32, 38). Both protein and mRNA levels were measured. Tethering Def1 to the mRNA through either the N- or C-terminus of Def1 led to significant reduction of both GFP mRNA- and protein levels relative to the free MCP control (Fig. 3B and C). Both protein and mRNA were reduced approximately 40-50%, but not quite to the magnitude of repression conferred by the Dhh1-MCP control. These results suggest that Def1 has a direct function in the regulation of mRNAs.

Def1 acts like other factors implicated in both decay and synthesis of mRNAs. Previous studies have shown that tethering mRNA decay(1) or general transcription factors(39) to promoters can activate transcription. We therefore, constructed fusion proteins of the DNA binding domain of LexA and different fragments of Def1 (Full length and 1-380). A LexA-TBP, TATA-binding protein was analyzed in parallel. Whereas, the LexA-TBP fusion activated the reporter gene, neither LexA-Def1 proteins did (Supplementary Fig. S3C). However, this tethering assay reports on the effects on preinitiation complex formation, and a negative result does not disprove Def1's effect on transcription, such as at elongation.

Def1 associates with polyribosomes

Def1-TID labelled proteins involved in translation (Fig. 2B and C). Translation and RNA decay are coupled processes(40–42). We therefore hypothesized that Def1 functions in translation and/or interacts with polyribosomes. We performed polysome profiling to determine if Def1 associates with polyribosomes and to evaluate if Def1 is required for global translation by measuring the polysome to monosome ratio (henceforth referred to as P/M ratio). Lysates from wild type cells were fractionated on 10-50% sucrose gradients and the fractions were probed with anti-Def1 antibodies. We found that the majority of Def1 migrates with the mono- and polyribosome fractions and comparatively little was in the mRNP fraction (Fig. 4A). Some Def1 was also detected in the fractions containing the 40S and 60S subunits. To verify that Def1 is associated with

polysomes, we prepared lysates and gradients in buffers containing EDTA, a polysome disassembling agent. EDTA treatment disrupted the migration of Def1 in the heavier polysome fractions (Fig. 4A), confirming that Def1 migrates with polyribosomes. Interestingly, Def1 still migrated with the 40- and 60S peaks, suggesting it interacts with the small and large subunits of the ribosome independent of translation.

The association of a protein with ribosomes implies that it influences translation. We examined the effects of deleting *DEF1* on translation by first calculating the polysome-to-monosome ratio (P/M) in the polysome profiles. When the polysome profiles of wildtype and *def1Δ* cells were overlaid, there was no striking differences in the 40S, 60S and 80S peaks or the polysome fractions. The polysome-to-monosome ratio (P/M) was not significantly affected by the loss of *DEF1* (Fig. 4B). We next examined if deleting *DEF1* caused sensitivity to the translation inhibitor hygromycin B, and indeed found that the *def1Δ mutant* was indeed sensitive to hygromycin B (Fig. 4C).

Puromycin incorporation into polypeptides is used to measure translation (43, 44). We therefore estimated protein synthesis by examining puromycin incorporation in wildtype and *def1Δ* strains, and found a significant reduction (~2.5-fold) in puromycin incorporation in the mutant (Fig. 4D). Thus, even though no change in polysome to monosome ratio was observed in the mutant cells, these results suggest Def1 is important for translation. More evidence for Def1's importance in translation is suggested by the upregulation of the steady state levels of mRNAs of ribosome biogenesis and translation factors in the *def1*Δ mutant (Supplementary Fig. S1A and B). These results can be interpreted as the mutant cells sensing impaired translation and upregulating pathways that respond to translation stress.

Ribosome sequencing (Ribo-seq) reveals a function of *DEF1* in translation

Bulk polysome profiling can mask changes in translation status, such as transcript-specific regulation, initiation-elongation dynamics and ribosome-dwelling kinetics Thus, we turned to ribosome-sequencing (ribo-seq) to detect translation changes in Δ*def1* cells. Ribosome-protected footprints (RPF) and mRNA reads of over 12 million (wild type) and over 19 million (*def1*Δ) were mapped to 5094 transcripts. Ribo-seq data was analyzed using the RiboMiner toolset (45). The three replicates of each experimental condition

correlated well and clustered together in PCA plots, and the RPFs showed a strong 3-nucleotide periodicity, a hallmark of ribo-seq. (Supplementary Fig. 4A, B).

Metaplots of ribosome distribution across mRNAs were centered over the start and stop codons (Fig. 5A and B, respectively). Ribosome density peaked over the start and stop codons in both cell types, as expected. However, RPFs were strikingly reduced between codons 30-45 and a small increase in density was detected over the start codon in the *def1*Δ mutant (Fig. 5A). The same pattern was observed when the metaplots were constructed normalizing to ORF length, indicating the reduction is not driven by a change in short ORFs (Supplementary Fig. 4C). No obvious difference in the RPFs was detected near the stop codon, but there was an unexplained spike in the mutant about 100 codons upstream of the stop codon. Another method to reveal shifts in ribosome density across mRNAs is a polarity plot, where a negative and positive score indicates a bias towards the 5' and 3' end, respectively. We found that the *def1*Δ mutant displayed a shift in the density of ribosome footprints towards the 3' end, having a more positive value (Fig. 5C). Based on the metaplot analysis, the shift appears to be driven by the reduced RPFs at the first 30-40 codons more so than an increase further down the transcript. The reduction in density occurs over the amino acid number found in the ribosome peptide exit channel (46, 47). The complex pattern could be explained by Def1p stabilizing ribosomes as the polypeptide moves through the exit channel, perhaps by inhibiting premature translation termination. The density recovery into the gene and a slight increase in density is observed at the 3' end in the mutant, which could result from the slowed elongation of ribosomes escaping termination. Slowed elongation would explain the reduced puromycin incorporation in the mutant (Fig. 4D).

We next examined changes in translation efficiency (TE) which is ribosome density on a specific message corrected for its mRNA levels. However, the increase in the TE of mRNAs can be caused by increased translation or ribosome stalling, because ribo-seq measures ribosome density and not necessarily translation per se. Of all 5094 mRNAs, 155 and 31 transcripts showed increased and decreased TE, respectively, when a cutoff of >1.5-FC and $p<0.005$ was applied (Fig. 5D). GO term analysis of the 155 mRNAs showed enrichment for genes regulating macromolecule metabolism

pathways (Supplementary Fig. S4D). No specific terms were associated with mRNAs with reduced TE.

Next, we examined if Def1 affects ribosome dwelling over specific codons. Some factors associated with Def1, for example, Ccr4-Not, regulate ribosome arrest over non-optimal codons(20, 48). We separated codons based on their codon stabilization coefficient (CSC) into three equal bins: high, intermediate and low codon optimality and then calculated the relative codon occupancy in the A-site mutant cells versus wild type cells (Fig. 5E). Strikingly, we found a significant increase in A-site occupancy in the mutant for the intermediate and non-optimal groups compared to the optimal codon group. (Fig. 5E). Plotting the change in ribosome density to specific codons demonstrated an overall mild increase in density of most codons, but consistent with the box plots in Fig. 5E, most non-optimal codons displayed increased A-site occupancy in the mutant (Supplementary Fig S4E). The data suggests that Def1 increases the ability of the ribosome to translate less optimal codons.

Def1 binding to polysomes requires its ubiquitin binding domain

We examined which region of Def1 is required for ribosome binding. Def1 contains an N-terminal CUE domain that interacts with ubiquitin-homology domains and ubiquitin(6) and a C-terminal polyglutamine-rich domain (polyQ) that is required for its accumulation in the cytoplasm (Fig. 6A). We generated a strain that expressed a truncation mutant of Def1 ($Def1_{1-380}$) lacking the polyQ region by incorporating GFP into the C-terminus. Full-length Def1-GFP (1-738) was also generated as a control. The 1-380 mutant retained ribosome binding, and moreover, we reproducibly observed enhanced polysome binding, especially in the heavier (larger) polysome fraction (Fig. 6B). One explanation for increased polysome interaction in the polyQ truncation mutant could be that bioinformatic tools predict a large intrinsically disorder segment within the polyQ region (data not shown), and Def1 forms polyQ-dependent amyloid-like filaments *in vitro* (49). A portion of full-length Def1 may be trapped in an insoluble fraction in cells and liberating the N-terminus from the polyQ domain may increase the amount available to bind ribosomes. Another explanation is that the polyQ region recruits factors that affect translation elongation.

Since $Def1_{1-380}$ associates with ribosomes, we hypothesized that the ubiquitin-binding CUE domain is responsible for this activity. We used CRISPR-Cas9 gene editing to introduce two clusters of mutations in the CUE domain, Cue1mut and Cue2mut, that disrupts Def1 binding to ubiquitin and ubiquitin-homology domains(6). Using strains that express these mutant versions of Def1 ($Def1_{CUE1}$ and $Def1_{CUE1,2}$ double mutant), we found that mutating the CUE domain, and likely ubiquitin binding, greatly reduced Def1's association with ribosomes (Fig. 6C). Furthermore, unlike what was observed in wild type extracts, the majority of mutant Def1 appears in the mRNP fractions. Interestingly, when the polysome profiles of the mutants were overlayed with the wild type, two differences were noted. First, the P/M ratio increased modestly in both CUE mutants, ~2.9 in mutants versus ~2.3 in wild type extracts (Fig. 6C), and the second, the amount of monosomes and polysomes were decreased (Fig. 6C). It should be noted that the amount of 40S and 60S subunits were not different between the wild type and the mutants, suggests that translation initiation may be impaired in the CUE mutants. These results were unexpected, considering no difference in polysome profiles in the wild-type strain and the *def1*Δ mutant was observed (Fig. 4C). This can be explained by the CUE mutants acting in a dominant negative manner, titrating translation factors away from ribosome (see below).

We screened the *DEF1* mutants for the sensitivity to the translation elongation inhibitor hygromycin. The strain expressing Def1(1-380) was similarly sensitive to hygromycin B as the *def1Δ* strain (Fig. 6D). Likewise, the CUE mutant strains showed sensitivity to the translation inhibitor, but less than the null mutant (Fig. 6D versus 4C). The CUE mutants required a high concentration to completely stop growth compared to the deletion mutant. These results indicate that Def1 association with ribosomes requires its CUE domain and ubiquitin-binding.

Not4-mediated ubiquitylation of eS7a (Rps7A) is required for the association of Def1 with polyribosomes

Ubiquitylation of ribosomal proteins (RPs) plays several roles in translation, such as rescuing stalled ribosomes and destroying aberrant nascent polypeptides by the ribosome quality control (RQC) pathway(50). Based on our findings that the CUE

domain of Def1 is necessary for its association with polysomes, we hypothesized that ubiquitylation of a RP plays a role in its recruitment. There are multiple ubiquitin ligases that carry out modification of RPs, and one is the Not4 subunit of the Ccr4-Not complex(19–21, 50, 51). As described above, BioID indicates that Def1 and Ccr4-Not are near each other (Fig. 2) and Def1 and Not4 have genetic and physical interactions(8, 18). Not4 ubiquitylates eS7A (Rps7A) in arrested ribosomes, such as those at non-optimal codons (20, 21, 50)Click or tap here to enter text..

We determined if Ccr4-Not, Not4 specially, is required for Def1 binding to ribosomes. Not1 is the scaffold subunit of the complex, and is encoded by an essential gene. Thus, we used auxin-induced degron strategy to deplete it from cells (Fig. 7A) (25). Depleting Not1 caused a remarkable reduction in the association of Def1 with ribosomes and a shift into the mRNP fraction (Fig 7B). Deleting the entire *NOT4* coding sequence or depleting the protein by auxin-dependent degradation also disrupted Def1's association with polyribosomes (Supplementary Fig S5B and C). Next, we examined if the ubiquitin ligase activity of Not4 is required for Def1 recruitment to ribosomes by analyzing a Not4 RING domain deletion mutant (*not4ring*Δ) that disrupts ubiquitin ligase activity, but leaves the Ccr4-Not complex otherwise intact(18). Here too we found that Def1 association with ribosomes was greatly reduced, indicating that the ubiquitin-ligase activity of Not4 is responsible for Def1 binding to ribosomes (Fig. 7C).

Although these results indicate that Ccr4-Not, the ubiquitin ligase activity of Not4 specifically, recruits Def1 to ribosomes, they only suggest it is mediated by eS7A (Rps7A) ubiquitylation. These results could be ascribed to a secondary effect resulting from disruption of other Not4 RING-dependent functions or Not4's modification of other ribosome associated proteins. To directly link eS7A ubiquitylation to the recruitment of Def1 to polyribosomes, we utilized a yeast strain that contains lysine to arginine substitutions in the Not4-dependent ubiquitylation sites (eS7A-4KR)(20). We observed a striking loss of Def1 association with ribosomes in the mutant and increased amounts in the mRNP fraction, which mimicked the *not4ΔRING* condition (Fig. 7C and D). This result further supports our conclusion that Not4-mediated ubiquitylation of eS7a precedes the recruitment of Def1 and demonstrates that ubiquitin signaling is important in the recruitment of Def1 to polyribosomes.

Def1 recruits the translation control factor, Dhh1 to ribosomes

The C-terminus of Def1 retains it in the cytoplasm and progressively deleting the polyQ domain phenocopies the deletion mutant ((6) and Supplementary Fig. S6A). We hypothesized that the polyQ region recruits proteins to ribosomes to impact translation or co-translational decay. To test this, we generated strains expressing versions of Def1 fused to TID with progressive truncations of its C-terminus; $Def1_{1-380}$, $Def1_{1-500}$ and $Def1_{1-530}$. BioID was conducted on these strains. A growth spot assay showed that fusing TID to full length Def1 did not result in slowed growth or sensitivity to DNA damaging agents, but shortening the C-terminus phenocopied the deletion mutant (Supplementary Fig. S6A). The expression levels of all Def1-TID fusions were equivalent (Supplementary Fig. 6B). As an initial qualitative check of the biotin-transfer activities of the different mutants, we examined the levels of biotinylated proteins enriched on streptavidin beads by probing these fractions with streptavidin-horseradish peroxidase (HRP). There were some differences in the number and intensity of biotinylated proteins, but strong biotinylation was observed for all derivatives except for the $Def1_{1-500}$ -TID fusion protein, which labeled proteins to a lesser extent (Supplementary Fig. S6C). Mass spectrometry identified 59 enriched proteins labeled by the $Def1_{1-500}$ mutants, even though this crude analysis of labeled proteins suggested lower activity. Both $Def1_{1-530}$ and $Def1_{1-380}$ TID fusion proteins labeled a few more interacting partners than the full-length protein, labeling 105 and 120 versus 93, respectively (Fig. 8A). Interestingly, when we compared the percentage of targets labeled by the Def1 derivates that are posttranscriptional RNA regulators or RNA binding proteins, we found that those lacking the polyQ region labeled less RNA regulators than the full length Def1-TID protein. (Fig. 8A). Compared to the 34 (37% of total) labelled RNA regulators by the full-length protein, the $Def1_{1-380}$, $Def1_{1-500}$ and $Def1_{1-530}$ proteins labeled, 17 (14%), 10 (17%) and 14 (13%), respectively (Fig. 8A).

The loss of interaction of RNA regulators with the truncated versions of Def1 suggests that the C-terminus recruits factors to the ribosome. We therefore scanned the BioID dataset to identify an interacting protein that might play a role in ribosome dynamics or mRNA degradation. Notably, we found the DEAD box RNA helicase Dhh1,

which is a translation repressor and involved in co-translational mRNA decay(32, 52, 53), was labeled by the full-length protein, but not the truncated proteins. We performed polysome profiling to determine if the association of Dhh1 with polysomes is Def1-dependent. Dhh1 was found to associate with polyribosomes and was more enriched in the early polysome fractions, as described by others (Fig. 8B)(32). This might be explained by Dhh1's role in clearing ribosomes from mRNA during repression as ribosomes stalling increases throughout the body. Importantly, Dhh1 migration with polyribosomes was lost in the *def1*Δ mutant (Fig. 8B). This suggests that Def1 recruits Dhh1 to ribosomes.

It was recently reported that Dhh1 association with ribosomes required Not4 (see supplement of reference (20). Considering that Not4-dependent ubiquitylation is required for Def1 association, we verified this result and indeed found that that Dhh1 interaction with polyribosomes was reduced in the *not4*Δ mutant (Fig. 8C). Likewise, Not4 depletion by AID-dependent proteolysis diminished the association of Dhh1 with polyribosomes (data not shown).

Finally, to establish an order of events, we examined if Dhh1 is required for Def1 binding to polysomes. We carried out polysome profiling on *dhh1Δ* mutant lysates and observed that Def1 still migrated with polysomes in the absence of Dhh1, confirming that Def1 recruitment precedes that of Dhh1 (Fig 8D). Finally, we determined if directly tethering $Def1_{1\text{-}380}$, $Def1_{1\text{-}500}$ to the GFP reporter mRNA caused repression in the MS2/MCP assay. We found that the truncation mutants were not as effective as the wild type Def1-MCP fusion protein at suppressing expression of the reporter construct (Supplementary Figure S6D and E). These results suggest that Def1 acts as a ubiquitin-dependent scaffold or adaptor protein to link translation status to downstream events such as co-translational mRNA decay.

Discussion

An ever-growing number of genes are found to have novel or underappreciated activities. For example, Ccr4-Not once thought only to control TBP and transcription initiation, is now recognized for its important functions in posttranscriptional control of mRNAs. Degradation factor 1, Def1, was first identified as a DNA damage mitigating

factor, and a substantial amount of work has established it as an elongation and a degradation factor that clears arrested RNA polymerase II (RNAPII) from genes. Other nuclear functions have been attributed to Def1(8). Despite its presence in the cytoplasm, no cytoplasmic functions had been identified. Here, we characterized a new function for Def1 in the cytoplasm, post-transcriptional gene control.

DEF1 controls RNA synthesis and decay rates. Def1 is an RNAPII elongation factor that co-purified with TFIIH and affects start site selection in reconstituted transcription reactions(8, 49). Thus, its role in maintaining synthesis rates was expected, but not so for its requirement for normal mRNA decay. Even though transcript buffering could have accounted for the slowed mRNA decay in a *def1*Δ mutant due to perturbed transcription, we provide evidence that Def1 controls posttranscriptional gene regulation, probably by associating with polyribosomes. Def1 is associated with many cytoplasmic posttranscriptional regulators that bind to polyribosomes and the MS2/MCP reporter assay suggests it directly regulates mRNA, versus the change in decay resulting from buffering of reduced synthesis. Considering that a large amount of decay occurs co-translationally, it is likely Def1's ability to recruit decay factors to ribosomes affects decay (42) .

Our work reconciles the perplexing cytoplasmic localization and the very high abundance of Def1. Estimates of median abundance for Def1 cited in the *Saccharomyces cerevisiae* database (SGD) is ~21,000, but the estimate can be as high as 80,000. As noted above, DNA damage causes the proteasomal processing of a fraction of Def1, but a larger fraction of unprocessed protein remains in the cytoplasm(6). Def1 has cytoplasmic functions and its presence there serves a purpose greater than preventing it from prematurely entering the nucleus and interfering with transcription. Def1 has transcription functions, but it also has important cytoplasmic functions. As such, Def1 adds to a list of factors involved in transcription in the nucleus and translation/decay in the cytoplasm. Ccr4-Not, which we describe as an initiator of Def1 recruitment to ribosomes, connects transcription elongation to translation(20, 54). Def1, too, may be important for nuclear-cytoplasmic communication by coordinating transcription and translation.

We propose a model where Not4-dependent ubiquitylation of eS7a recruits Def1 to ribosomes through Def1's CUE domain, where it, in turn, recruits regulators of translation and/or decay through its C-terminal region (Fig. 9). Interestingly, we found reduced monosome and polysome abundance in cells expressing the ubiquitin-binding mutants (CUEmut1,2), but not in the deletion mutant (Fig. 6C). The reason for this is unclear, but we speculate that the CUE domain mutant may act as a dominant negative by sequestering or titrating away a translation factor from ribosomes. The CUE mutant retains the polyQ-rich segment that our BioID experiments suggests interacts with mRNA regulators.

What does Def1 do during translation? Although Def1 is associated with polyribosomes, deleting the gene had no detectable effect on the polysome profiles (Fig. 4). On the other hand, translation, as measured by puromycin incorporation and altered distribution of ribosome footprints across mRNAs suggests it affects translation. This could occur if overall translation rates from initiation to elongation are reduced. Ubiquitylation of ribosomal proteins affects multiple stages of translation. A clue to a mechanism comes from structural studies of the 43S preinitiation complex that predicts that eS7 ubiquitylation would disrupt eIF4A and eIF4G interaction with the ribosome(55) and deubiquitylation of eS7 is required to allow the cap-binding complex eIF4F to bind to the 43S complex (56). Interestingly, subunits of eIF4A are labeled by Def1-TID (Fig. 2 and Supplemental file 3). Furthermore, eIF3 straddles both sides of eS7, and cycles of eS7 ubiquitylation and deubiquitylation would lead to the recruitment and disassociation of Def1. In this regard, Def1 senses the translation status of mRNAs. Future studies, well beyond the scope of this work, on the structure of Def1 bound to ribosomes may provide additional insights.

Ribo-seq studies revealed increased ribosome dwelling over non-optimal codons in the A-site in the null mutant, which is consistent with the role of Ccr4-Not in sensing ribosomes arrested over these codons during elongation(50, 56–59). A unique phenotype of the *def1*Δ mutant, compared to *not4*Δ and *not5*Δ mutants, however, is that ribosome density is diminished over ~30-40 codons in the *def1*Δ mutant. This is the length of the peptide in the RNA exit tunnel (60). mRNA fate is determined by its nascent polypeptide and associated factors (61). Def1 may play a role similar to the

nascent polypeptide complex (NAC). NAC prevents SRP from mislocalizing cytoplasmic proteins and aids to delaying protein folding in a chaperone-like manner by inserting a domain in the tunnel(62). Interestingly, the Egd2 subunit of NAC contains a ubiquitin-like domain (UBLs). The CUE domain of Def1 also binds UBLs. Furthermore, Not4 affects the ubiquitylation and function of NAC(63), once again connecting the function of Not4 and Def1 to ribosome function. Def1 binding to ribosomes may prevent early termination by premature recruitment of quality control factors early in the mRNA, which could involve coordinating NAC activity.

Def1 interacts with ribonucleoprotein granules (RNPs) markers such as Ccr4-Not subunits, Edc3, Dhh1, Lsm7, and others. Ribonucleoprotein granules, such as stress granules and processing bodies, are cytosolic compartments for translational repression, whereby mRNAs are stored together with initiation factors and decay factors during stress (64). However, UV stress (6) or nutrient stress (data not shown) did not induce Def1-containing foci, such as P-bodies. Recently, the putative human homolog of Def1 was identified, UBAP2/2L(65). UBAP2/2L resides in and is required for stress granule formation(12, 66). Interestingly, UBAP2/2L co-sedimented with mammalian ribosomes, and knocking it down decreased translation(67). However, while UBAP2/2L has a ubiquitin-binding domain, it lacks the polyQ-rich domain found in Def1, so it was not known if Def1 had cytoplasmic functions or if UBAP2/2L acquired it. Although Def1 does not form detectable foci, it could regulate the partitioning of mRNAs between the repressed versus the actively translated pool. Not4/5 is important for partitioning mRNAs in the soluble and insoluble fraction(21).

Def1's nuclear and cytoplasmic functions may be connected. Agents that damage DNA and arrest RNA polymerase II also damage RNA and arrests ribosomes. RNA polymerase II degradation and Def1 processing is also triggered by transcriptional stress initiated by depleting GTP pools using 6-azauracil (6-AU) and mycophenolic acid(6). GTP is essential for ribosome movement, and 6-AU treatment causes ribosomes to accumulate on mRNAs(54). Like RNAPII detects DNA damage as it moves along the gene, ribosomes can sense untranslatable mRNAs and trigger ribosome quality control pathways (50). It would be advantageous for cells to sense untranslatable mRNAs in the cytoplasm and shut down transcription, or the newly made

transcripts would meet the same fate. It is feasible that Def1 senses and plays a role in shutting down gene expression at multiple levels in response to nucleic acid damage.

In addition to its well-characterized role in resolving DNA-damage arrested RNA polymerase II, Def1 has other nuclear functions associated with genomic integrity mechanisms (for review see (8).). One such function is the destruction of Pol3, the catalytic subunit of replicative DNA polymerase delta(68). The ubiquitylation and removal of Pol3 leads to the exchange of replicative for translesion DNA polymerase. Here, Def1 uses DNA polymerase to detect DNA damage and directs polymerase destruction, allowing for continued DNA replication by translesion DNA polymerase. We propose the exciting idea that Def1 acts as a ubiquitin-dependent scaffold protein that plays a role in surveying the activity of molecular motors that scan nucleic acids for damage. Def1 is well connected to molecular motors that scan DNA, such as DNA and RNA polymerase II and now RNA, the ribosome. In this capacity, Def1 plays an essential role in ubiquitin-mediated signaling to resolve damage to cells and guard the genome from errors.

Acknowledgements:
Mass Spectrometry was performed by Dr. Tatiana Laremore at the Penn State Huck Proteomics and Mass Spectrometry Core Facility (RRID:SCR_024462). The Genomics Research Incubator (RRID:SCR_024530) and Genomics (RRID:SCR_023645) cores of the Huck Institutes of Life Science were used in this work. We thank Fred Winston, Jeff Coller and Toshifumi Inada for providing plasmids and strains. Karen Arndt is recognized for sharing the nascent transcription protocol. Rachael Green is acknowledged for input on metagene plots of RPFs. This research was supported by funds from National Institutes of Health (R35 GM136353 to J.C.R).

Data availability: Genomics data has been deposited to GEO under accession number GSE290861. Proteomics data will be uploaded to MassIVE.

References:

1. Haimovich,G., Choder,M., Singer,R.H. and Trcek,T. (2013) The fate of the messenger is pre-determined: a new model for regulation of gene expression. *Biochim Biophys Acta*, **1829**, 643–53.
2. Sun,M., Schwalb,B., Pirkl,N., Maier,K.C., Schenk,A., Failmezger,H., Tresch,A. and Cramer,P. (2013) Global analysis of eukaryotic mRNA degradation reveals Xrn1-dependent buffering of transcript levels. *Mol Cell*, **52**, 52–62.
3. Timmers,H.T.M. and Tora,L. (2018) Transcript Buffering: A Balancing Act between mRNA Synthesis and mRNA Degradation. *Mol Cell*, **72**, 10–17.
4. Haimovich,G., Medina,D.A., Causse,S.Z., Garber,M., Millán-Zambrano,G., Barkai,O., Chávez,S., Pérez-Ortín,J.E., Darzacq,X. and Choder,M. (2013) Gene expression is circular: factors for mRNA degradation also foster mRNA synthesis. *Cell*, **153**, 1000–11.
5. Reese,J.C. (2013) The control of elongation by the yeast Ccr4-not complex. *Biochim Biophys Acta*, **1829**, 127–33.
6. Wilson,M.D., Harreman,M., Taschner,M., Reid,J., Walker,J., Erdjument-Bromage,H., Tempst,P. and Svejstrup,J.Q. (2013) Proteasome-mediated processing of Def1, a critical step in the cellular response to transcription stress. *Cell*, **154**, 983–995.
7. Steurer,B. and Marteijn,J.A. (2017) Traveling Rocky Roads: The Consequences of Transcription-Blocking DNA Lesions on RNA Polymerase II. *J Mol Biol*, **429**, 3146–3155.
8. Akinniyi,O.T. and Reese,J.C. (2021) DEF1: Much more than an RNA polymerase degradation factor. *DNA Repair (Amst)*, **107**, 103202.
9. Reese,J.C. (2023) New roles for elongation factors in RNA polymerase II ubiquitylation and degradation. *Biochim Biophys Acta Gene Regul Mech*, **1866**, 194956.
10. Woudstra,E.C., Gilbert,C., Fellows,J., Jansen,L., Brouwer,J., Erdjument-Bromage,H., Tempst,P. and Svejstrup,J.Q. (2002) A Rad26-Def1 complex coordinates repair and RNA pol II proteolysis in response to DNA damage. *Nature*, **415**, 929–33.
11. Somesh,B.P., Reid,J., Liu,W.-F., Søgaard,T.M.M., Erdjument-Bromage,H., Tempst,P. and Svejstrup,J.Q. (2005) Multiple mechanisms confining RNA polymerase II ubiquitylation to polymerases undergoing transcriptional arrest. *Cell*, **121**, 913–23.
12. Youn,J.-Y., Dunham,W.H., Hong,S.J., Knight,J.D.R., Bashkurov,M., Chen,G.I., Bagci,H., Rathod,B., MacLeod,G., Eng,S.W.M., *et al.* (2018) High-Density Proximity Mapping Reveals the Subcellular Organization of mRNA-Associated Granules and Bodies. *Mol Cell*, **69**, 517-532.e11.
13. Pfannenstein,J., Tyryshkin,M., Gulden,M.E., Doud,E.H., Mosley,A.L. and Reese,J.C. (2024) Characterization of BioID tagging systems in budding yeast and exploring the interactome of the Ccr4-Not complex. *G3 (Bethesda)*, **14**.
14. Miller,J.E. and Reese,J.C. (2012) Ccr4-Not complex: the control freak of eukaryotic cells. *Crit Rev Biochem Mol Biol*, **47**, 315–33.
15. Collart,M.A. (2016) The Ccr4-Not complex is a key regulator of eukaryotic gene expression. *Wiley Interdiscip Rev RNA*, **7**, 438–54.
16. Chalabi Hagkarim,N. and Grand,R.J. (2020) The Regulatory Properties of the Ccr4-Not Complex. *Cells*, **9**.

17. Kruk,J.A., Dutta,A., Fu,J., Gilmour,D.S. and Reese,J.C. (2011) The multifunctional Ccr4-Not complex directly promotes transcription elongation. *Genes Dev*, **25**, 581–93.
18. Jiang,H., Wolgast,M., Beebe,L.M. and Reese,J.C. (2019) Ccr4-Not maintains genomic integrity by controlling the ubiquitylation and degradation of arrested RNAPII. *Genes Dev*, **33**, 705–717.
19. Panasenko,O.O. and Collart,M.A. (2012) Presence of Not5 and ubiquitinated Rps7A in polysome fractions depends upon the Not4 E3 ligase. *Mol Microbiol*, **83**, 640–53.
20. Buschauer,R., Matsuo,Y., Sugiyama,T., Chen,Y.H., Alhusaini,N., Sweet,T., Ikeuchi,K., Cheng,J., Matsuki,Y., Nobuta,R., *et al.* (2020) The Ccr4-Not complex monitors the translating ribosome for codon optimality. *Science (1979)*, **368**.
21. Allen,G.E., Panasenko,O.O., Villanyi,Z., Zagatti,M., Weiss,B., Pagliazzo,L., Huch,S., Polte,C., Zahoran,S., Hughes,C.S., *et al.* (2021) Not4 and Not5 modulate translation elongation by Rps7A ubiquitination, Rli1 moonlighting, and condensates that exclude eIF5A. *Cell Rep*, **36**, 109633.
22. Brachmann,C.B., Davies,A., Cost,G.J., Caputo,E., Li,J., Hieter,P. and Boeke,J.D. (1998) Designer deletion strains derived from Saccharomyces cerevisiae S288C: a useful set of strains and plasmids for PCR-mediated gene disruption and other applications. *Yeast*, **14**, 115–32.
23. Laughery,M.F., Hunter,T., Brown,A., Hoopes,J., Ostbye,T., Shumaker,T. and Wyrick,J.J. (2015) New vectors for simple and streamlined CRISPR-Cas9 genome editing in Saccharomyces cerevisiae. *Yeast*, **32**, 711–20.
24. Longtine,M.S., McKenzie,A., Demarini,D.J., Shah,N.G., Wach,A., Brachat,A., Philippsen,P. and Pringle,J.R. (1998) Additional modules for versatile and economical PCR-based gene deletion and modification in Saccharomyces cerevisiae. *Yeast*, **14**, 953–61.
25. Shetty,A., Reim,N.I. and Winston,F. (2019) Auxin-Inducible Degron System for Depletion of Proteins in Saccharomyces cerevisiae. *Curr Protoc Mol Biol*, **128**, e104.
26. Francette,A.M. and Arndt,K.M. (2024) Multiple direct and indirect roles of the Paf1 complex in transcription elongation, splicing, and histone modifications. *Cell Rep*, **43**, 114730.
27. Love,M.I., Huber,W. and Anders,S. (2014) Moderated estimation of fold change and dispersion for RNA-seq data with DESeq2. *Genome Biol*, **15**, 550.
28. Neymotin,B., Athanasiadou,R. and Gresham,D. (2014) Determination of in vivo RNA kinetics using RATE-seq. *RNA*, **20**, 1645–52.
29. Zenklusen,D., Larson,D.R. and Singer,R.H. (2008) Single-RNA counting reveals alternative modes of gene expression in yeast. *Nat Struct Mol Biol*, **15**, 1263–71.
30. Vijjamarri,A.K., Gupta,N., Onu,C., Niu,X., Zhang,F., Kumar,R., Lin,Z., Greenberg,M.L. and Hinnebusch,A.G. (2023) mRNA decapping activators Pat1 and Dhh1 regulate transcript abundance and translation to tune cellular responses to nutrient availability. *Nucleic Acids Res*, **51**, 9314–9336.
31. McGlincy,N.J. and Ingolia,N.T. (2017) Transcriptome-wide measurement of translation by ribosome profiling. *Methods*, **126**, 112–129.
32. Sweet,T., Kovalak,C. and Coller,J. (2012) The DEAD-box protein Dhh1 promotes decapping by slowing ribosome movement. *PLoS Biol*, **10**, e1001342.

33. Rose,M. and Botstein,D. (1983) Structure and function of the yeast URA3 gene. Differentially regulated expression of hybrid beta-galactosidase from overlapping coding sequences in yeast. *J Mol Biol*, **170**, 883–904.
34. Kim,D.I., Jensen,S.C., Noble,K.A., Kc,B., Roux,K.H., Motamedchaboki,K. and Roux,K.J. (2016) An improved smaller biotin ligase for BioID proximity labeling. *Mol Biol Cell*, **27**, 1188–96.
35. Kim,D.I. and Roux,K.J. (2016) Filling the Void: Proximity-Based Labeling of Proteins in Living Cells. *Trends Cell Biol*, **26**, 804–817.
36. Kulkarni,S., Morrissey,A., Sebastian,A., Giardine,B., Smith,C., Akinniyi,O.T., Keller,C.A., Arnaoutov,A., Albert,I., Mahony,S., *et al.* (2024) Human CCR4-NOT globally regulates gene expression and is a novel silencer of retrotransposon activation. *bioRxiv*, 10.1101/2024.09.10.612038.
37. Branon,T.C., Bosch,J.A., Sanchez,A.D., Udeshi,N.D., Svinkina,T., Carr,S.A., Feldman,J.L., Perrimon,N. and Ting,A.Y. (2018) Efficient proximity labeling in living cells and organisms with TurboID. *Nat Biotechnol*, **36**, 880–887.
38. Zeidan,Q., He,F., Zhang,F., Zhang,H., Jacobson,A. and Hinnebusch,A.G. (2018) Conserved mRNA-granule component Scd6 targets Dhh1 to repress translation initiation and activates Dcp2-mediated mRNA decay in vivo. *PLoS Genet*, **14**, e1007806.
39. Chatterjee,S. and Struhl,K. (1995) Connecting a promoter-bound protein to TBP bypasses the need for a transcriptional activation domain. *Nature*, **374**, 820–2.
40. Hu,W., Sweet,T.J., Chamnongpol,S., Baker,K.E. and Coller,J. (2009) Co-translational mRNA decay in Saccharomyces cerevisiae. *Nature*, **461**, 225–9.
41. Bae,H. and Coller,J. (2022) Codon optimality-mediated mRNA degradation: Linking translational elongation to mRNA stability. *Mol Cell*, **82**, 1467–1476.
42. Wu,Q. and Bazzini,A.A. (2023) Translation and mRNA Stability Control. *Annu Rev Biochem*, **92**, 227–245.
43. Cary,G.A., Yoon,S.H., Torres,C.G., Wang,K., Hays,M., Ludlow,C., Goodlett,D.R. and Dudley,A.M. (2014) Identification and characterization of a drug-sensitive strain enables puromycin-based translational assays in Saccharomyces cerevisiae. *Yeast*, **31**, 167–78.
44. Enam,S.U., Zinshteyn,B., Goldman,D.H., Cassani,M., Livingston,N.M., Seydoux,G. and Green,R. (2020) Puromycin reactivity does not accurately localize translation at the subcellular level. *Elife*, **9**.
45. Li,F., Xing,X., Xiao,Z., Xu,G. and Yang,X. (2020) RiboMiner: a toolset for mining multi-dimensional features of the translatome with ribosome profiling data. *BMC Bioinformatics*, **21**, 340.
46. Wilson,D.N., Arenz,S. and Beckmann,R. (2016) Translation regulation via nascent polypeptide-mediated ribosome stalling. *Curr Opin Struct Biol*, **37**, 123–33.
47. Dao Duc,K. and Song,Y.S. (2018) The impact of ribosomal interference, codon usage, and exit tunnel interactions on translation elongation rate variation. *PLoS Genet*, **14**, e1007166.
48. Müller,M.B.D., Becker,T., Denk,T., Hashimoto,S., Inada,T. and Beckmann,R. (2025) The ribosome as a platform to coordinate mRNA decay. *Nucleic Acids Res*, **53**.

49. Damodaren,N., Van Eeuwen,T., Zamel,J., Lin-Shiao,E., Kalisman,N. and Murakami,K. (2017) Def1 interacts with TFIIH and modulates RNA polymerase II transcription. *Proc Natl Acad Sci U S A*, **114**, 13230–13235.
50. Inada,T. and Beckmann,R. (2024) Mechanisms of Translation-coupled Quality Control. *J Mol Biol*, **436**, 168496.
51. Ikeuchi,K., Tesina,P., Matsuo,Y., Sugiyama,T., Cheng,J., Saeki,Y., Tanaka,K., Becker,T., Beckmann,R. and Inada,T. (2019) Collided ribosomes form a unique structural interface to induce Hel2-driven quality control pathways. *EMBO J*, **38**.
52. Coller,J. and Parker,R. (2005) General translational repression by activators of mRNA decapping. *Cell*, **122**, 875–86.
53. Radhakrishnan,A., Chen,Y.-H., Martin,S., Alhusaini,N., Green,R. and Coller,J. (2016) The DEAD-Box Protein Dhh1p Couples mRNA Decay and Translation by Monitoring Codon Optimality. *Cell*, **167**, 122-132.e9.
54. Gupta,I., Villanyi,Z., Kassem,S., Hughes,C., Panasenko,O.O., Steinmetz,L.M. and Collart,M.A. (2016) Translational Capacity of a Cell Is Determined during Transcription Elongation via the Ccr4-Not Complex. *Cell Rep*, **15**, 1782–94.
55. Brito Querido,J., Sokabe,M., Díaz-López,I., Gordiyenko,Y., Fraser,C.S. and Ramakrishnan,V. (2024) The structure of a human translation initiation complex reveals two independent roles for the helicase eIF4A. *Nat Struct Mol Biol*, **31**, 455–464.
56. Takehara,Y., Yashiroda,H., Matsuo,Y., Zhao,X., Kamigaki,A., Matsuzaki,T., Kosako,H., Inada,T. and Murata,S. (2021) The ubiquitination-deubiquitination cycle on the ribosomal protein eS7A is crucial for efficient translation. *iScience*, **24**, 102145.
57. Matsuda,H., Putzel,G.G., Backman,V. and Szleifer,I. (2014) Macromolecular crowding as a regulator of gene transcription. *Biophys J*, **106**, 1801–10.
58. Yan,L.L. and Zaher,H.S. (2019) Ubiquitin-a beacon for all during quality control on the ribosome. *EMBO J*, **38**.
59. Yan,L.L. and Zaher,H.S. (2019) How do cells cope with RNA damage and its consequences? *J Biol Chem*, **294**, 15158–15171.
60. Wilson,D.N., Arenz,S. and Beckmann,R. (2016) Translation regulation via nascent polypeptide-mediated ribosome stalling. *Curr Opin Struct Biol*, **37**, 123–33.
61. Höpfler,M. and Hegde,R.S. (2023) Control of mRNA fate by its encoded nascent polypeptide. *Mol Cell*, **83**, 2840–2855.
62. Gamerdinger,M. and Deuerling,E. (2024) Cotranslational sorting and processing of newly synthesized proteins in eukaryotes. *Trends Biochem Sci*, **49**, 105–118.
63. Panasenko,O., Landrieux,E., Feuermann,M., Finka,A., Paquet,N. and Collart,M.A. (2006) The yeast Ccr4-Not complex controls ubiquitination of the nascent-associated polypeptide (NAC-EGD) complex. *J Biol Chem*, **281**, 31389–98.
64. Van Treeck,B. and Parker,R. (2018) Emerging Roles for Intermolecular RNA-RNA Interactions in RNP Assemblies. *Cell*, **174**, 791–802.
65. Herlihy,A.E., Boeing,S., Weems,J.C., Walker,J., Dirac-Svejstrup,A.B., Lehner,M.H., Conaway,R.C., Conaway,J.W. and Svejstrup,J.Q. (2022) UBAP2/UBAP2L regulate UV-induced ubiquitylation of RNA polymerase II and are the human orthologues of yeast Def1. *DNA Repair (Amst)*, **115**, 103343.

66. Sanders,D.W., Kedersha,N., Lee,D.S.W., Strom,A.R., Drake,V., Riback,J.A., Bracha,D., Eeftens,J.M., Iwanicki,A., Wang,A., *et al.* (2020) Competing Protein-RNA Interaction Networks Control Multiphase Intracellular Organization. *Cell*, **181**, 306-324.e28.
67. Luo,E.-C., Nathanson,J.L., Tan,F.E., Schwartz,J.L., Schmok,J.C., Shankar,A., Markmiller,S., Yee,B.A., Sathe,S., Pratt,G.A., *et al.* (2020) Large-scale tethered function assays identify factors that regulate mRNA stability and translation. *Nat Struct Mol Biol*, **27**, 989–1000.
68. Daraba,A., Gali,V.K., Halmai,M., Haracska,L. and Unk,I. (2014) Def1 promotes the degradation of Pol3 for polymerase exchange to occur during DNA-damage--induced mutagenesis in Saccharomyces cerevisiae. *PLoS Biol*, **12**, e1001771.

Figure legends:

Figure 1: **DEF1 is required for mRNA synthesis and decay.** (A). Total RNA-seq was carried out in both wild type (WT) and *def1Δ* strains in replicate. DEseq2 was used to determine changes in expression. *S. pombe* spike-in was used at 1:14 OD ratio of cells to normalize the data. Upregulated transcripts (>2-fold change, p_{adj}<0.01) appear in red and downregulated transcripts (<2-fold change, p_{adj}<0.01) appear in blue. (B). RNA synthesis rates are reduced in the *def1*Δ mutant. RATE-seq was used to determine global RNA synthesis rates. Rates obtained for the 3596 transcripts that overlap in the wild type and *def1*Δ samples are displayed in the figure. *p* value was determined using an unpaired *t*-test. (C). *DEF1* globally controls mRNA decay rates. As in "B", except decay rates were plotted. (D). GO term analysis of the processes associated with the top quartile (Q4) transcripts whose decay rates change the most in the mutant.
(E). Evidence for transcript buffering in the *def1*Δ mutant. Scatterplot of the fold change (FC) in RNA decay and synthesis rates were plotted on the y- and x-axis, respectively. A Spearman correlation coefficient is shown in the scatterplot.

Figure 2: BioID analysis reveals that Def1 interacts with posttranscriptional regulatory factors. (A). BioID labeling was performed in cells expressing Def1-Turbo ID (TID) and cells expressing free TID enzyme. Biological replicates were analyzed. Biotinylated proteins were pulled down using streptavidin beads and identified by mass spectrometry. Data is presented as a Volcano plot of fold change of protein abundance ratio (Def1-TID versus free TID) versus p-value. The enriched proteins (>1.5fold, p<0.05) appear in red and underrepresented proteins (<1.5fold, p<0.05) appear in blue. Proteins enriched in the Def1-TID sample were analyzed using ShinyGO 0.80 and the enriched process (B), component (C) and function (D) are shown.

Figure 3: **MS2-MCP Reporter assays indicate that Def1 functions in posttranscriptional control of mRNAs.** (A) Schematic of the MS2 coat protein (MCP)-MS2 tethering assay. (B). Graph of steady-state GFP mRNA. RT-qPCR measured the abundance of both GFP and *ACT1* (control) mRNA. GFP mRNA amounts were

normalized to *ACT1*. The relative abundance of GFP mRNA in the fusion protein-expressing cells, compared to that expressing free MCP protein, was set at 1.0 (N=3). Def1-MCP has MCP fused to the C-terminus; MCP-Def1 has MCP fused to the N-terminus; Dhh11-MCP was used as a positive control. Expression of the free MCP and the Def1-MCP fusion proteins were driven by the *DEF1* promoter (see methods). Dhh1-MCP was driven by the *DHH1*-promoter. (C). Analysis of GFP protein abundance. GFP protein expression level was determined by Western blotting using anti-GFP antibody. Taf14 was used as a loading control and GFP protein signals were normalized to the control (N=3).

Figure 4: **Def1 associates with polyribosomes and is required for translation.** (A). Ribosome profiling. Cell lysate was fractionated on a 10-50% sucrose gradient as described in the Methods section. A_{254} recording of the gradient fractions are displayed in the chart. Def1 and Rpl3-s (large subunit protein) were detected by Western blotting. The locations of the mRNP, 40S, 60S, 80S monosomes and polysomes are indicated. Fractionation of Def1 in the presence (red) or absence (black) of the polysome disrupting agent EDTA. Two blots were used to analyze all the fractions and the splice is indicated with white space. (B). Representative polysome profiles of wild type and *def1Δ* cells overlayed (wild type cells in black and *def1Δ* in red). The average polysome-to-monosome ratios (P/M) were determined and represented in the table. The area under the curve (AUC) for the monosome (80S) and polysome fractions were calculated using PeakChart 3 software (Brandel). The average and standard deviations (N=3) are shown. (C) *DEF1* null cells are sensitive to translation inhibitor, hygromycin B. Cells were spotted onto YPAD media and the same with 50 ug/ml hygromycin. Images captured at 24- and 48-hr. (D) Puromycin incorporation is impaired in *def1*Δ. Cells were grown to log phase and puromycin was added for 15 min prior to harvesting. Western blot of cell extracts using anti-puromycin antibodies detected puromycin incorporation. Results are the average and standard deviation (N=3).

Figure 5. Ribosome profiling (Ribo-seq) of the *def1*Δ mutant revealed altered ribosome distribution and increased non-optimal codons in the A-site. (A) Metaplot

analysis of ribosome density distribution over the first 150 codons of all 5140 transcripts. Metagene plots were generated using RiboMiner v0.2, ribosome density at each position is normalized by the overall ribosome density of coding sequence. Wild type (in blue) and *def1Δ* (in red) conditions are plotted. (B) Metaplot analysis as in *A*. The ribosome density distribution across 150 codons upstream of the stop codon of all ORFs. (C) Polarity Score of ribosome density across mRNAs. Transcriptome-wide shift in overall ribosome distribution was evaluated and represented for both wild type (in blue) and *def1Δ* mutant (in red). (D) Change in translation efficiency (TE) in a *def1*Δ mutant. (E). Change in ribosome density over the A-site versus codon optimality. Codons were separated into three bins based on CSC scores, optimal (n=20), intermediate (n=21) and non-optimal (n=20). Stop codons were not included in this analysis. The change in ribosome density over the A-site is plotted on a log2 scale. P-values were calculated using a 2-tail unpaired t-test.

Figure 6: **The N-terminus of Def1, the CUE domain specifically, binds ribosomes.** (A). Schematic of the Def1 protein with the poly-Q and CUE domains illustrated. (B). Def1(1-380)-GFP migration in polysome profiles. Western blot was performed using anti-GFP antibodies. (C). Polysome fractions of wild type, CUEmut1 and CUEmut1,2. The amino acid substitutions were described in Supplemental Table 1 and reference 6. Western blotting was performed using Def1 antiserum and Rpl3-s. (D) Hygromycin B (hygB) sensitivity growth assay. As in Fig 4C, except two concentrations of drug were used.

Figure 7. Ubiquitylation of eS7a by Not4 recruits Def1 to ribosomes. (A). Western blot showing Not1 depletion using the auxin-induced degron system. Antibodies to Not1 and Dhh1 (loading control) were used. Two isolates of the Not1-AID strain are shown. Cells were treated with auxin for 2 hr where indicated. (B). Lysates of untreated and auxin-treated Not1-AID cells were subjected to polysome analysis. Blots were probed with anti-Def1 and Rpl3-s antibodies. (C). Analysis of Def1 binding to polysomes in a *not4Δring* mutant. Blots were probed with anti-Def1 and Rpl3-s antibodies. (D). Lysates from strains expressing wild type eS7a or a version with lysine to arginine substitution in

the Not4-dependent ubiquitylation sites (eS7$_{KR}$ mut) (BUSCHAUER *et al.* 2020) were fractionated on sucrose gradients.

Figure 8. **The poly-glutamine-rich (polyQ) domain of Def1 mediates its interaction with mRNA regulators and recruits the decapping and translation regulator Dhh1 to ribosomes.** (A). BioID was conducted with Def1 truncation mutants fused to TID. Labeled proteins that were enriched for each Def1 derivative versus free TID (>1.5-fold, $p<0.05$) were tabulated. The number and percent of RNA regulators were calculated and displayed in the table. Dhh1 binding to ribosomes in a *def1*Δ (B) and *not4*Δ (C) mutants. (D). Def1 binding to ribosomes in a *dhh1*Δ mutant.

Figure 9. Model for Def1 recruitment to ribosomes. The model is based on reference 20**.** Ribosome arrest or stalling causes Not5 binding to the empty E-site, recruiting Ccr4-Not to the ribosome and causing eS7a ubiquitylation. Def1 binds ubiquitylated eS7a through its CUE domain and recruits RNA decay and translation factors to the ribosome through the C-terminal polyQ-rich domain. The CDC48 complex and the proteosome assist in ribosome quality control and ribosome removal.

Buschauer, R., Y. Matsuo, T. Sugiyama, Y. H. Chen, N. Alhusaini *et al.*, 2020 The Ccr4-Not complex monitors the translating ribosome for codon optimality. Science 368.

Figure 1

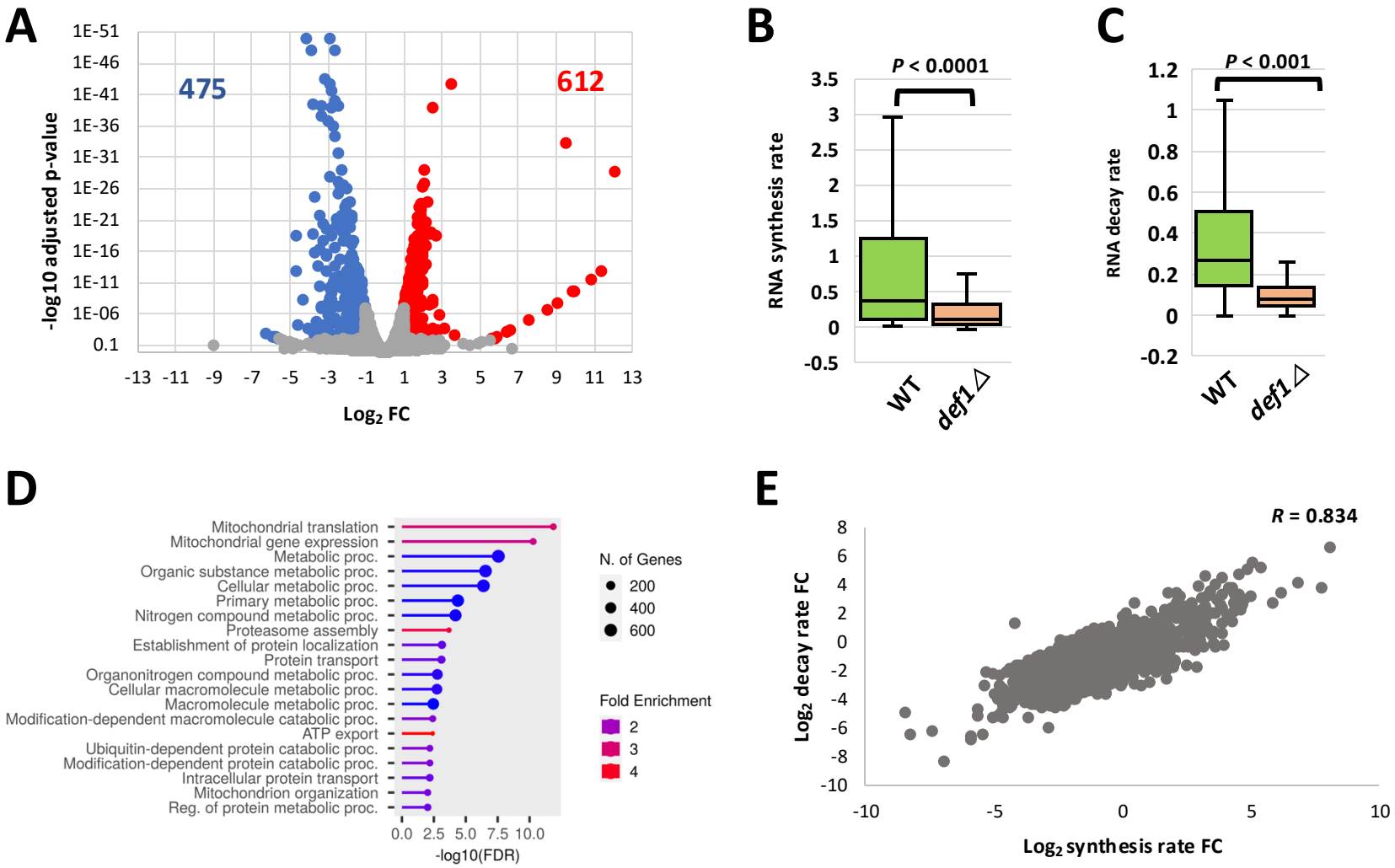
A
475
612
-log10 adjusted p-value
Log2 FC
B
P < 0.0001
RNA synthesis rate
WT
def1Δ
C
P < 0.001
RNA decay rate
WT
def1Δ
D
Mitochondrial translation
Mitochondrial gene expression
Metabolic proc.
Organic substance metabolic proc.
Cellular metabolic proc.
Primary metabolic proc.
Nitrogen compound metabolic proc.
Proteasome assembly
Establishment of protein localization
Protein transport
Organonitrogen compound metabolic proc.
Cellular macromolecule metabolic proc.
Macromolecule metabolic proc.
Modification-dependent macromolecule catabolic proc.
ATP export
Ubiquitin-dependent protein catabolic proc.
Modification-dependent protein catabolic proc.
Intracellular protein transport
Mitochondrion organization
Reg. of protein metabolic proc.
-log10(FDR)
N. of Genes
200
400
600
Fold Enrichment
2
3
4
E
R = 0.834
Log2 decay rate FC
Log2 synthesis rate FC

Figure 2

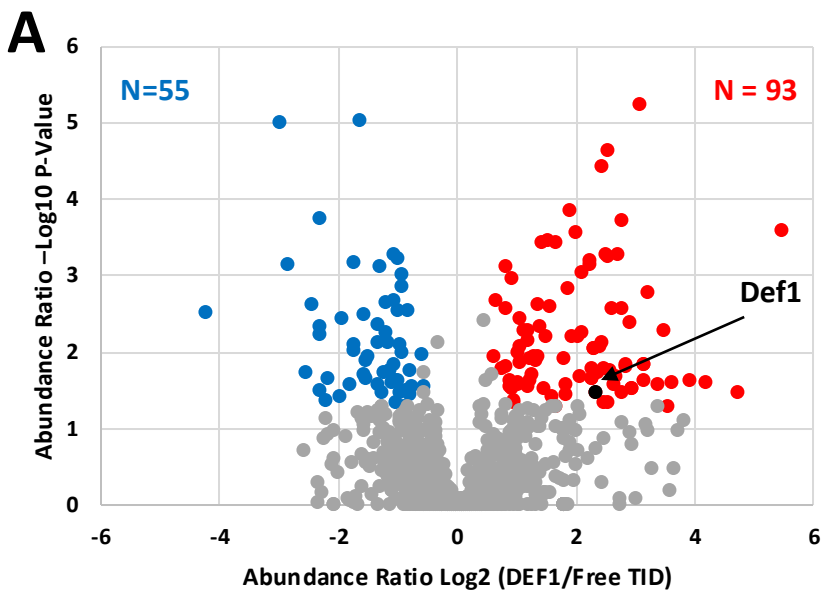
A
N=55
N = 93
Def1
Abundance Ratio –Log10 P-Value
Abundance Ratio Log2 (DEF1/Free TID)
6
5
4
3
2
1
0
-6
-4
-2
0
2
4
6

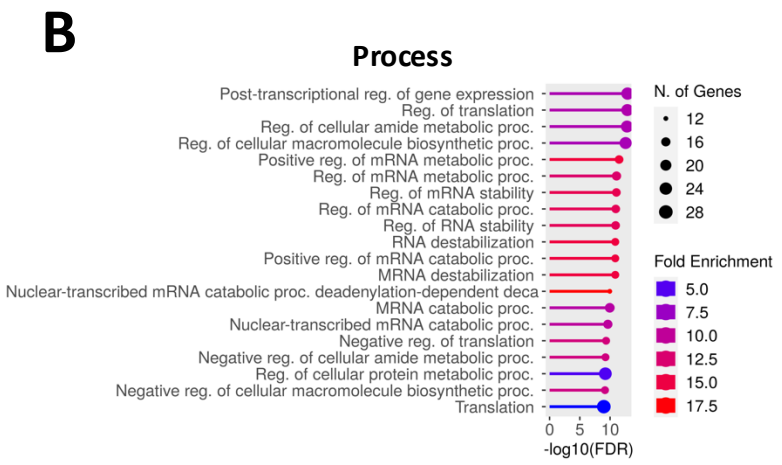
B
Process
Post-transcriptional reg. of gene expression
Reg. of translation
Reg. of cellular amide metabolic proc.
Reg. of cellular macromolecule biosynthetic proc.
Positive reg. of mRNA metabolic proc.
Reg. of mRNA metabolic proc.
Reg. of mRNA stability
Reg. of mRNA catabolic proc.
Reg. of RNA stability
RNA destabilization
Positive reg. of mRNA catabolic proc.
MRNA destabilization
Nuclear-transcribed mRNA catabolic proc. deadenylation-dependent deca
MRNA catabolic proc.
Nuclear-transcribed mRNA catabolic proc.
Negative reg. of translation
Negative reg. of cellular amide metabolic proc.
Reg. of cellular protein metabolic proc.
Negative reg. of cellular macromolecule biosynthetic proc.
Translation
0
5
10
-log10(FDR)
N. of Genes
12
16
20
24
28
Fold Enrichment
5.0
7.5
10.0
12.5
15.0
17.5

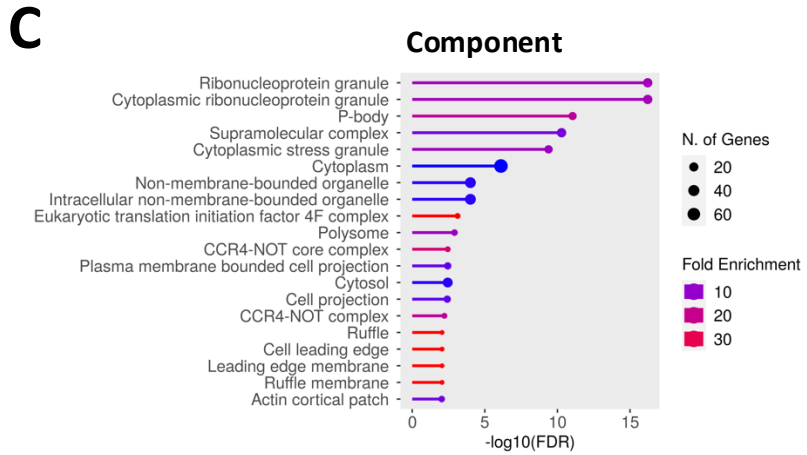
C
Component
Ribonucleoprotein granule
Cytoplasmic ribonucleoprotein granule
P-body
Supramolecular complex
Cytoplasmic stress granule
Cytoplasm
Non-membrane-bounded organelle
Intracellular non-membrane-bounded organelle
Eukaryotic translation initiation factor 4F complex
Polysome
CCR4-NOT core complex
Plasma membrane bounded cell projection
Cytosol
Cell projection
CCR4-NOT complex
Ruffle
Cell leading edge
Leading edge membrane
Ruffle membrane
Actin cortical patch
0
5
10
15
-log10(FDR)
N. of Genes
20
40
60
Fold Enrichment
10
20
30

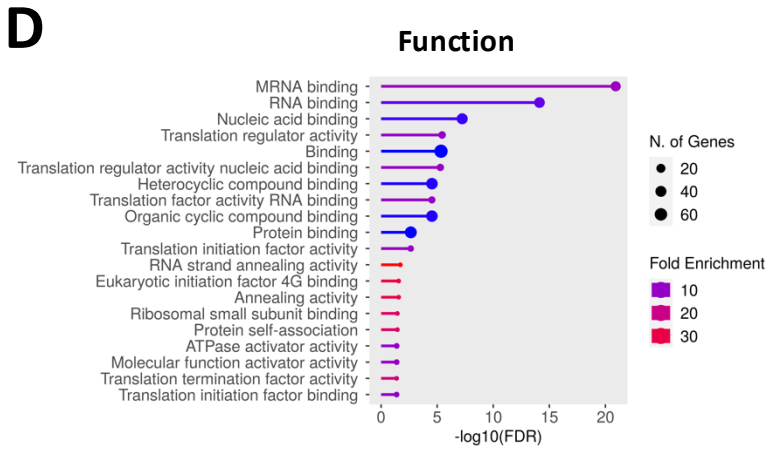
D
Function
MRNA binding
RNA binding
Nucleic acid binding
Translation regulator activity
Binding
Translation regulator activity nucleic acid binding
Heterocyclic compound binding
Translation factor activity RNA binding
Organic cyclic compound binding
Protein binding
Translation initiation factor activity
RNA strand annealing activity
Eukaryotic initiation factor 4G binding
Annealing activity
Ribosomal small subunit binding
Protein self-association
ATPase activator activity
Molecular function activator activity
Translation termination factor activity
Translation initiation factor binding
0
5
10
15
20
-log10(FDR)
N. of Genes
20
40
60
Fold Enrichment
10
20
30

Figure 3

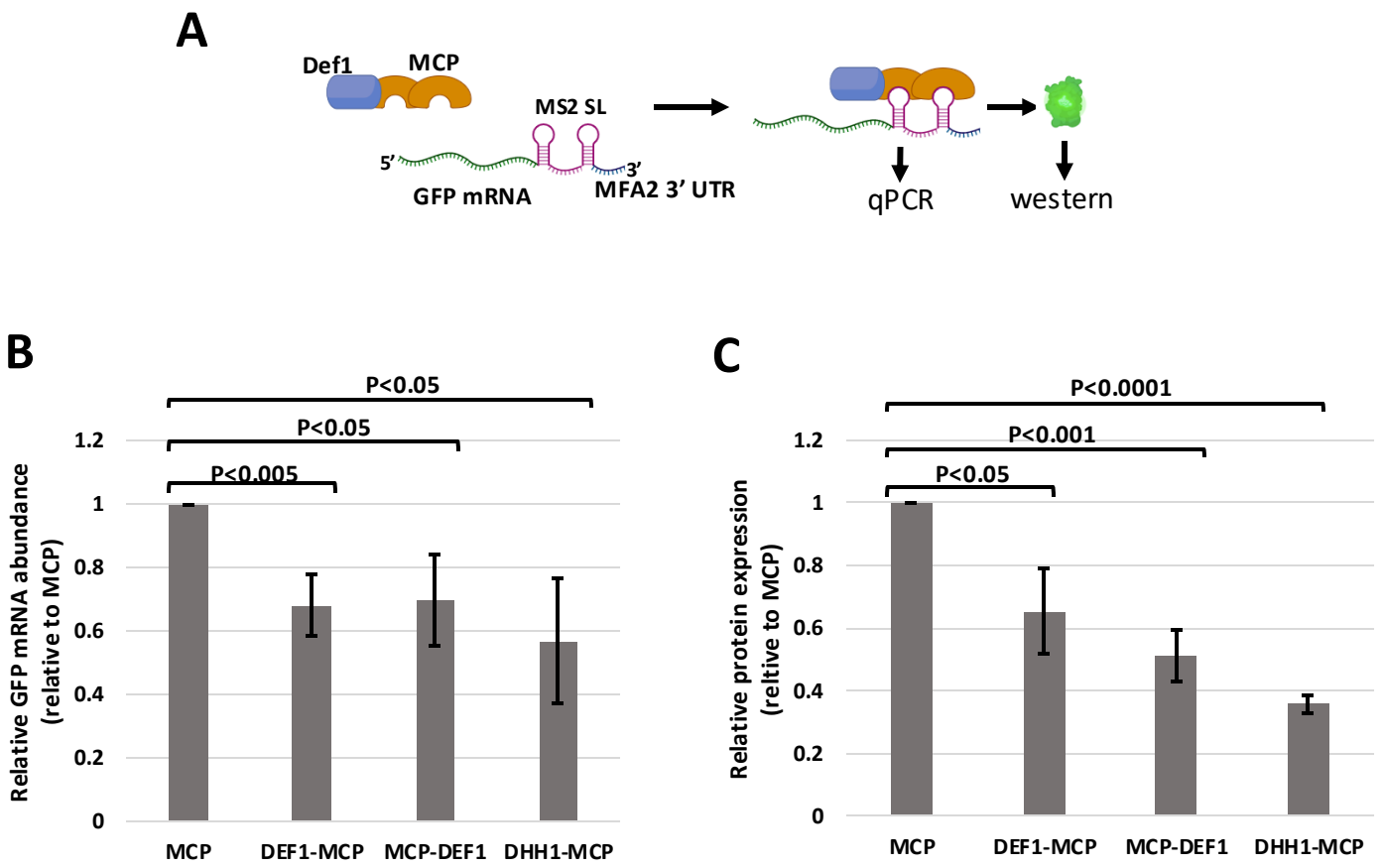
A
Def1
MCP
MS2 SL
5'
3'
GFP mRNA
MFA2 3' UTR
qPCR
western
B
P<0.05
P<0.05
P<0.005
Relative GFP mRNA abundance (relative to MCP)
1.2
1
0.8
0.6
0.4
0.2
0
MCP
DEF1-MCP
MCP-DEF1
DHH1-MCP
C
P<0.0001
P<0.001
P<0.05
Relative protein expression (reltive to MCP)
1.2
1
0.8
0.6
0.4
0.2
0
MCP
DEF1-MCP
MCP-DEF1
DHH1-MCP

Figure 4

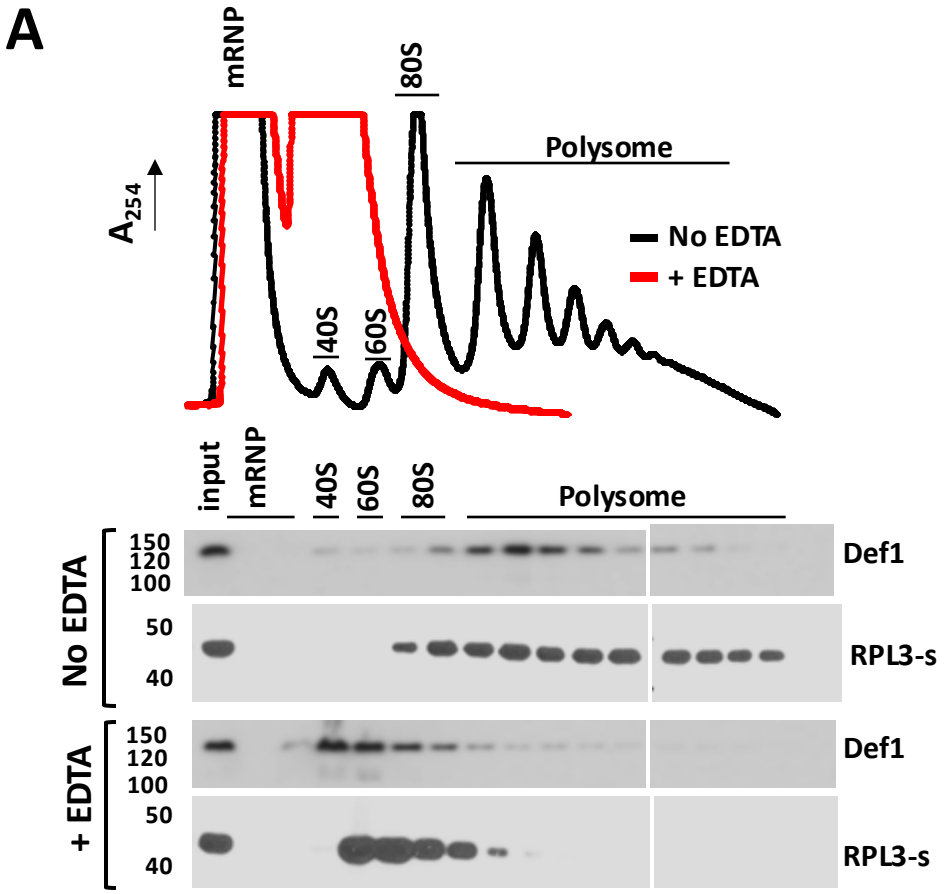

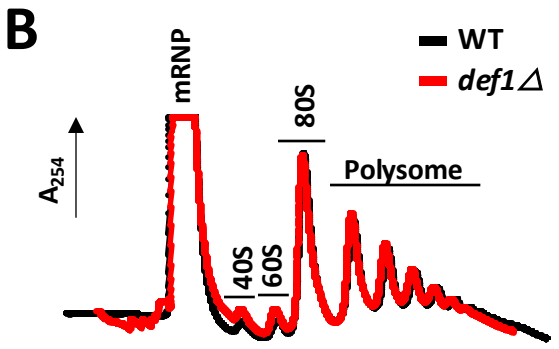

Condition	Average P/M ± SD
WT	2.23 ± 0.028
def1Δ	2.097 ± 0.119

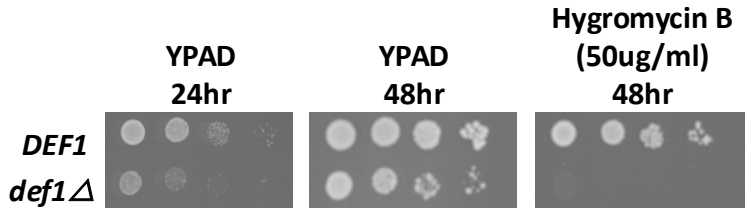

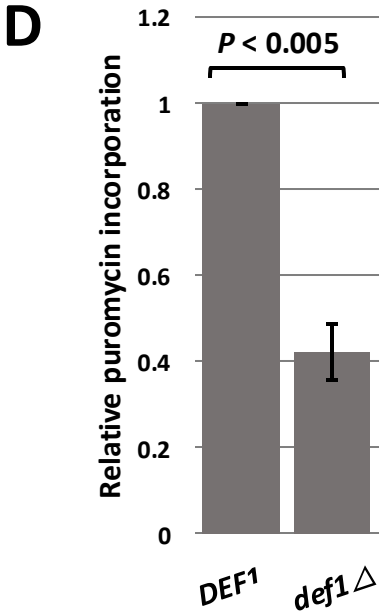

Figure 5

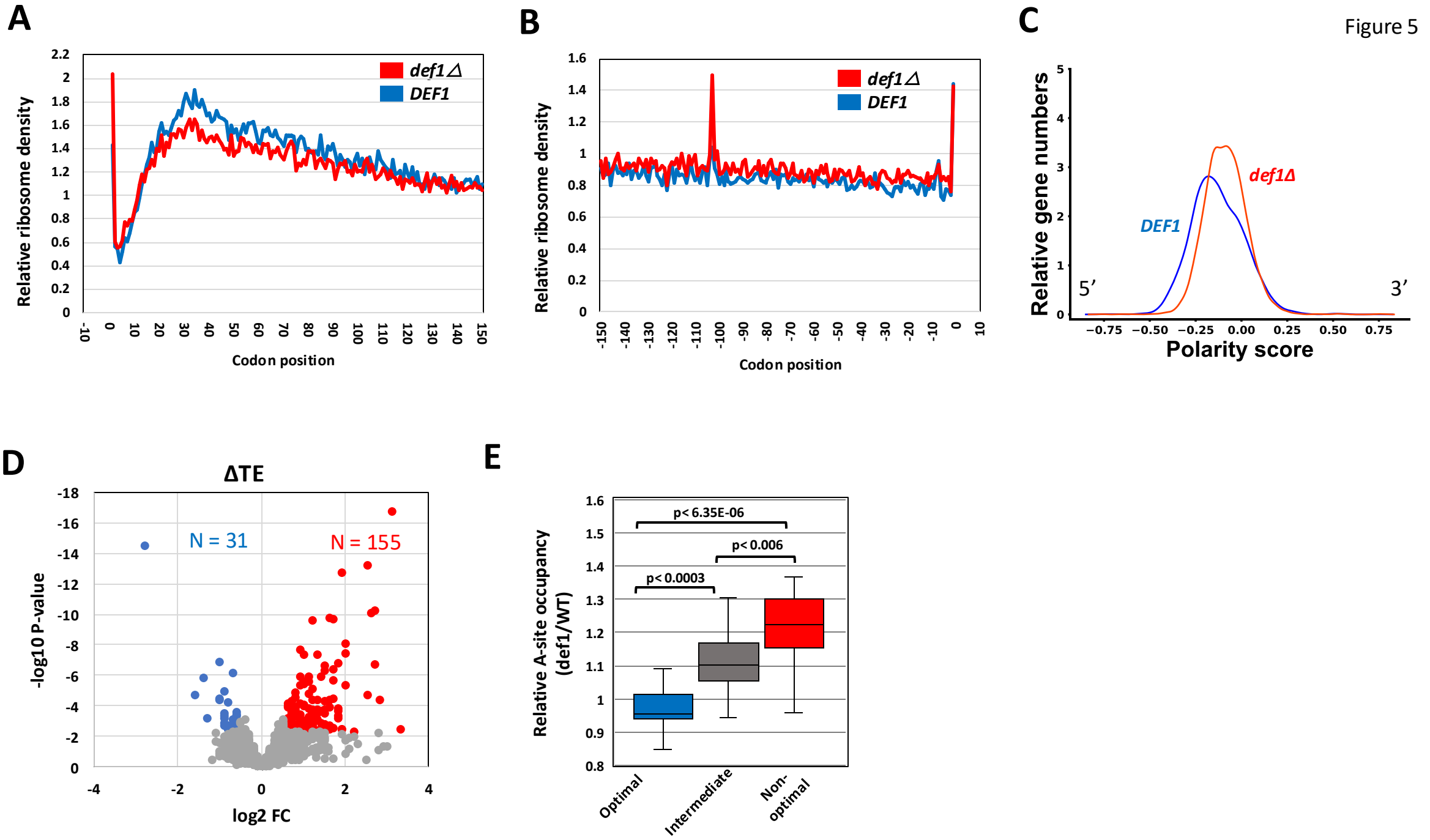
A
Relative ribosome density
Codon position
def1Δ
DEF1
B
Relative ribosome density
Codon position
def1Δ
DEF1
C
Relative gene numbers
Polarity score
def1Δ
DEF1
5'
3'
D
ΔTE
-log10 P-value
log2 FC
N = 31
N = 155
E
Relative A-site occupancy (def1/WT)
p< 6.35E-06
p< 0.006
p< 0.0003
Optimal
Intermediate
Non-optimal

Figure 6

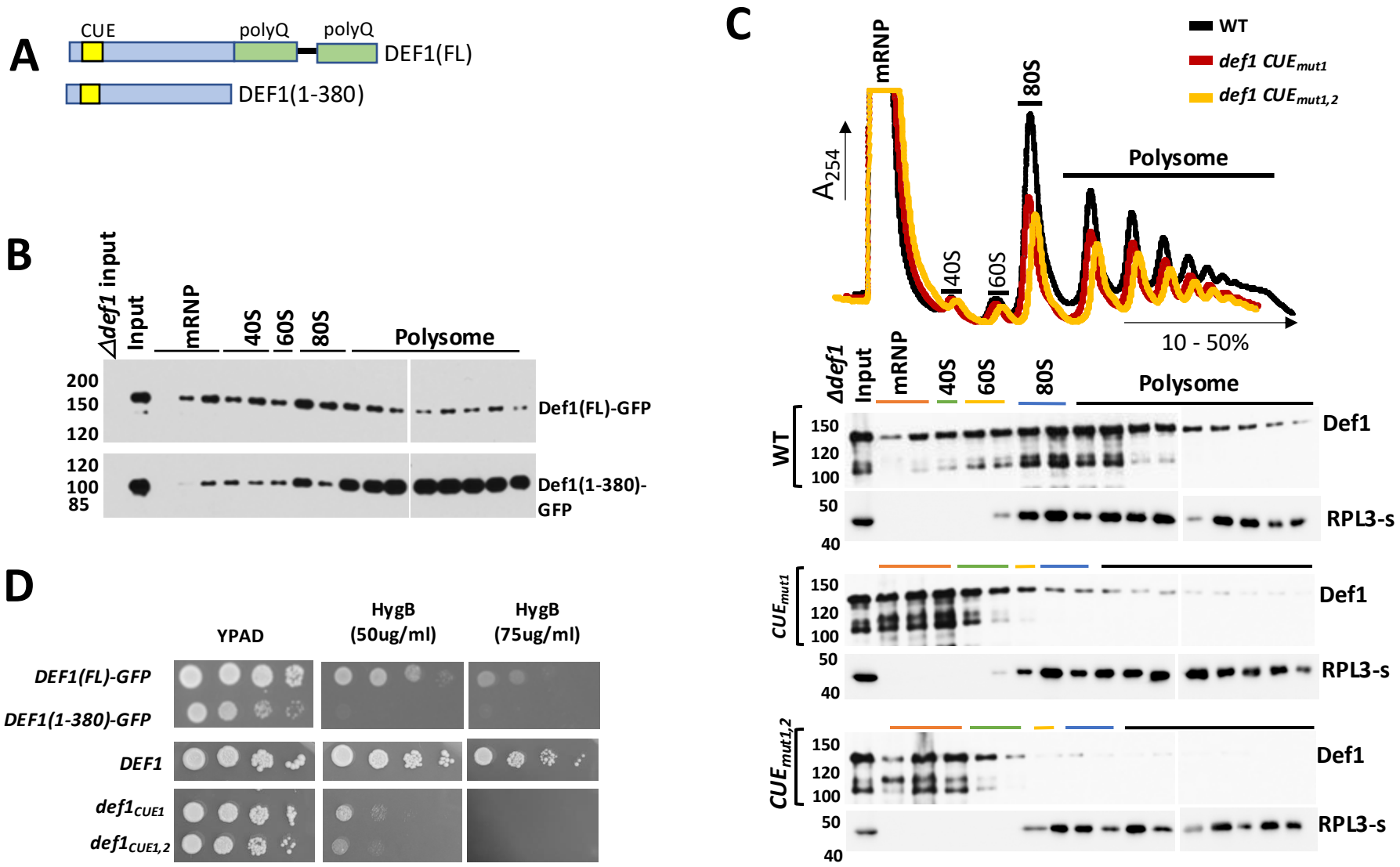
A
CUE
polyQ
polyQ
DEF1(FL)
DEF1(1-380)
B
Δdef1 input
Input
mRNP
40S
60S
80S
Polysome
200
150
120
Def1(FL)-GFP
120
100
85
Def1(1-380)-GFP
C
WT
def1 CUEmut1
def1 CUEmut1,2
mRNP
80S
40S
60S
Polysome
A254
10 - 50%
Δdef1
Input
mRNP
40S
60S
80S
Polysome
WT
150
120
100
Def1
50
40
RPL3-s
CUEmut1
Def1
RPL3-s
CUEmut1,2
Def1
RPL3-s
D
YPAD
HygB (50ug/ml)
HygB (75ug/ml)
DEF1(FL)-GFP
DEF1(1-380)-GFP
DEF1
def1CUE1
def1CUE1,2

Figure 7

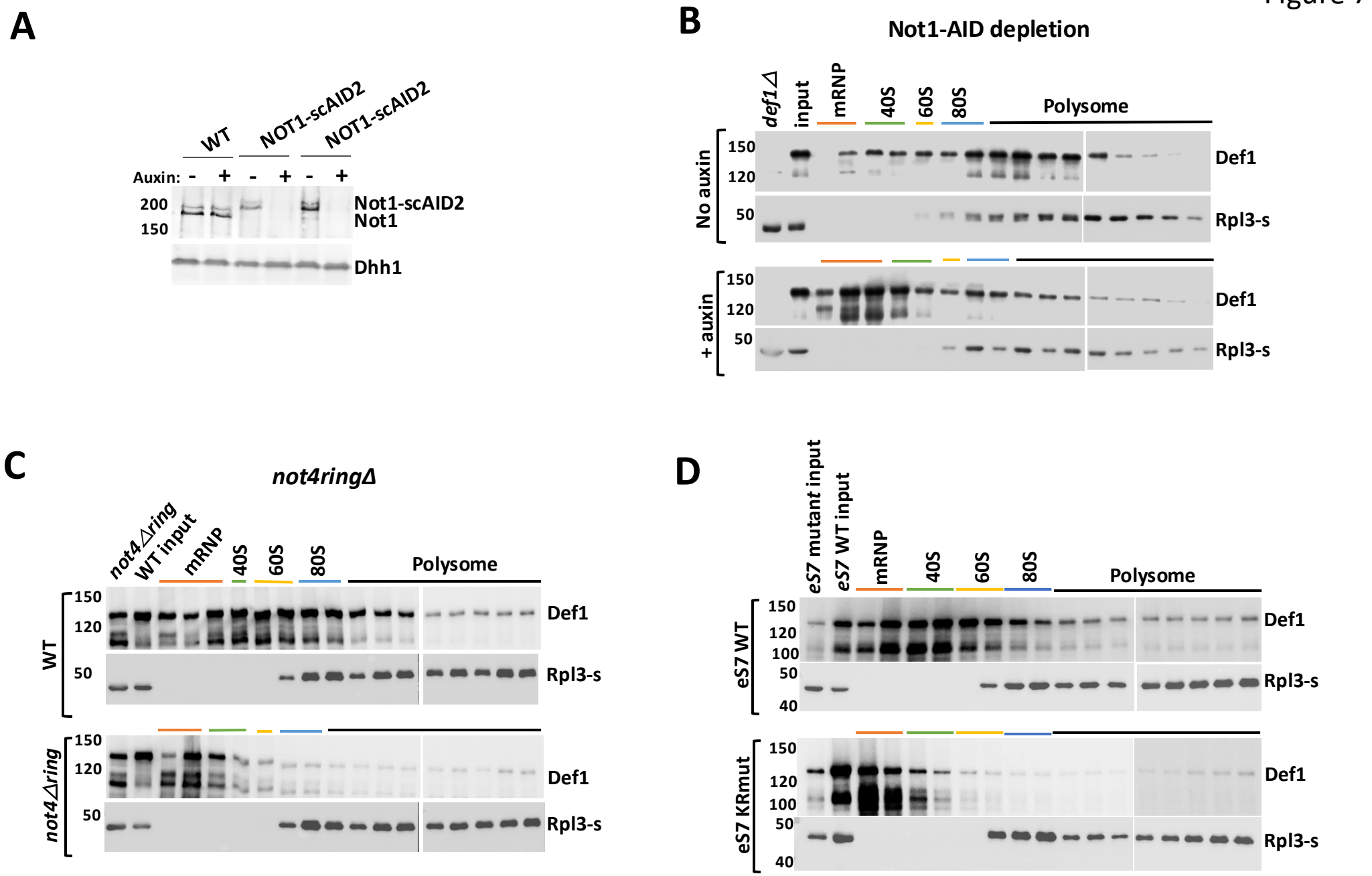
A
WT
NOT1-scAID2
NOT1-scAID2
Auxin: - + - + - +
200
150
Not1-scAID2
Not1
Dhh1
B
Not1-AID depletion
def1Δ
input
mRNP
40S
60S
80S
Polysome
No auxin
+ auxin
150
120
50
Def1
Rpl3-s
C
not4ringΔ
not4Δring
WT input
mRNP
40S
60S
80S
Polysome
WT
not4Δring
150
120
50
Def1
Rpl3-s
D
eS7 mutant input
eS7 WT input
mRNP
40S
60S
80S
Polysome
eS7 WT
eS7 KRmut
150
120
100
50
40
Def1
Rpl3-s

Figure 8

A.

TID fusion	labelled proteins	labelled RNA regulators (% of total labelled)
Def1(1-738)	93	34 (37%)
Def1(1-530)	105	14 (13%)
Def1(1-500)	59	10 (16.9%)
Def1(1-380)	120	17 (14%)

B.

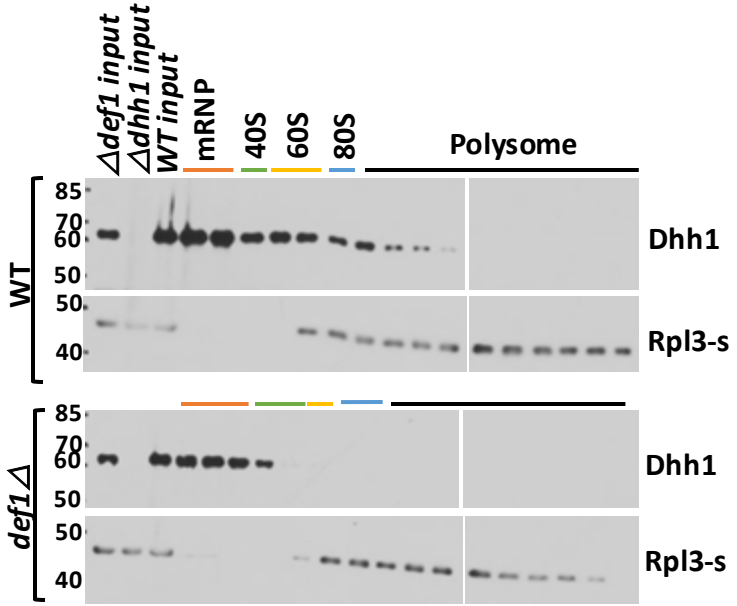

C.

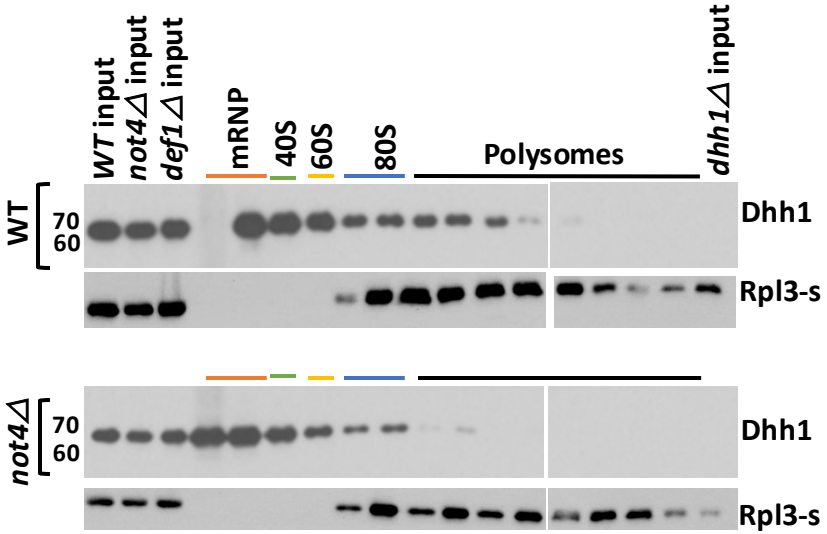

D.

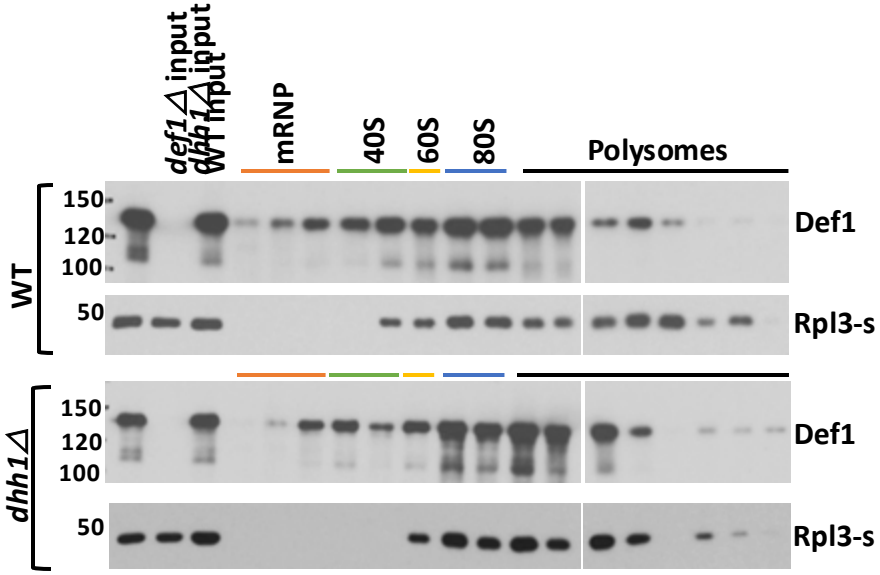

Figure 9

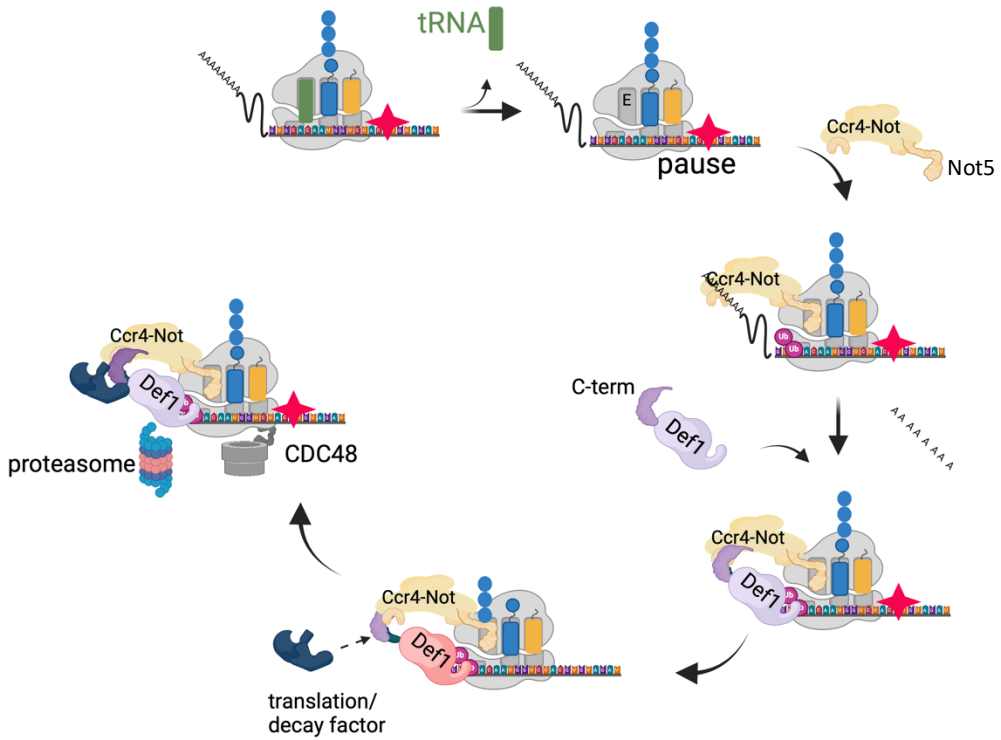
tRNA
E
pause
Ccr4-Not
Not5
Ccr4-Not
Ub
C-term
Def1
Ccr4-Not
Def1
Ccr4-Not
Def1
Ccr4-Not
Def1
proteasome
CDC48
translation/
decay factor